AN EVALUATION OF THE HOT-DRY-WINDY FIRE-WEATHER INDEX USING HISTORICAL FIRE EVENTS AND METEOROLOGICAL ANALYSIS DATASETS

 $\mathbf{B}\mathbf{y}$

McKenzie G. Kulseth

A THESIS

Submitted to
Michigan State University
in partial fulfillment of the requirements
for a degree of

 $Geography-Master\ of\ Science$

2019

ABSTRACT

AN EVALUATION OF THE HOT-DRY-WINDY FIRE-WEATHER INDEX USING HISTORICAL FIRE EVENTS AND METEOROLOGICAL ANALYSIS DATASETS

By

McKenzie G. Kulseth

This study evaluates the skill of a newly developed fire-weather index called the Hot-Dry-Windy Index (HDW) using five meteorological analysis datasets for twenty-three historical fire events, and sensitivities of that skill to assumptions made in index development. The meteorological analysis datasets used in this study are the Climate Forecast System Reanalysis, the Global Forecast System, the North American Regional Reanalysis, the Rapid Update Cycle, and the North American Mesoscale Forecast System. These datasets were chosen because they are widely used in weather forecast and other meteorological applications and because their data archives cover the period of historical fire events used in this study. The twenty-three historical wildland fire events were chosen to provide geographic diversity to this evaluation.

The results of this study suggest that the original HDW formulation is capable of identifying the largest fire spread day for between 56.5 to 78.3% of the twenty-three wildland fire events used in this study, and that alterations to the HDW formulation do not positively impact the skill of this index. The results also indicate that inclusion of the grid points surrounding the central-grid-point containing the latitude and longitude of each fire event in the evaluation of index skill provides higher skill than when only considering the central grid point. The skill of HDW computed by the five meteorological analysis datasets vary between fires and no one dataset consistently outperforms or underperforms the others.

I would like to dedicate this thesis to network of friends, and to my advisor a		
	Thank you	

ACKNOWLEDGEMENTS

I would like to thank my advisor, Sharon Zhong, my co-advisor and mentors Jay Charney, and my mentor Alan Srock for their support and encouragement during my time here at Michigan State University. I would also like to thank my third committee member Jeff Andresen, for his time and involvement in my graduate program. Their encouragement and guidance through life situations and keeping me on track is dearly appreciated. Furthermore, I want to especially thank my husband, Kyle Kulseth, for his kindness and support throughout this process, as well as my family and my friends. I could not have successfully completed this journey without all of you.

TABLE OF CONTENTS

LIST OF TABLES	vii
LIST OF FIGURES	viii
KEY TO ABBREVIATIONS	X
CHAPTER I – INTRODUCTION	1
CHAPTER II – LITERATURE REVIEW	5
1. Fire Weather Systems and Indices	5
1.1 Fire Danger Rating Systems	5
1.2 Fire Indices	
2. Summary	10
CHAPTER III – AN EVALUATION OF THE HOT-DRY-WINDY FIRE-VINDEX USING HISTORICAL FIRE EVENTS AND METEOROLOGICA DATASETS	L ANALYSIS 12
1. Introduction	
2. Data and Methods	14
2.1 Meteorological Analysis Datasets	14
2.2 Wildland Fire Events	16
2.3 Selecting the Largest Fire Spread Day	19
2.4 Evaluating HDW Skill	20
3. Sensitivity Testing	
4. Results	22
4.1 Distributions of HDW Values	22
4.2 Analysis Dataset Skill Comparisons	24
4.3 Layer Depth Sensitivities	27
4.4 Temporal Sensitivities	28
4.5 Combination of Layer Depth and Temporal Sensitivities	29
5. Discussion and Conclusion	30
CHAPTER IV – SUPPLIMENTARY RESULTS	32
1. Nine-Grid-Point Sensitivity to the Control	32
2. Layer Depth Sensitivities	33
2.1 Central-Grid-Point Analyses	33
2.2 Nine-Grid-Point Analyses	35
3. Temporal Sensitivities	
3.1 Central-Grid-Point Analyses	
3.2 Nine-Grid-Point Analyses	
4. Combination of Layer Depth and Temporal Sensitivities	
4.1 Central-Grid-Point Analyses	
4.2 Nine-Grid-Point Analyses	
4.3 Alternative Skill Evaluation of the Nine-Grid-Point Analyses	

CHAPTER V – THESIS CONCLUSIONS	51
BIBLIOGRAPHY	54

LIST OF TABLES

Table 1: Information for the five meteorological analysis datasets used in this study. Their names, abbreviations, and spatial and temporal resolutions are provided
Table 2: The names, abbreviations, locations, elevations, latitudes, longitudes, and date of largest fire spread of the twenty-three wildland fire events are provided
Table 3: The percentages of HDW successes for all wildland fire events using 1000-m and 1500-m layer depths to compare with the control analyses
Table 4: The percentages of HDW successes for all wildland fire events when using all available analysis dataset hours to compare with the control analyses
Table 5: Percentages of HDW successes for all wildland fire events for the sensitivities of HDW
Table 6: Alternative percentages of HDW successes for all wildland fire events when using three different temporal ranges depending on temporal resolution of each analysis dataset to compare with the control analyses

LIST OF FIGURES

Figure 1: Map presenting the locations of the twenty-three historical wildland fire events created using Google Earth Pro
Figure 2: A fire progression map for Pagami Creek fire event. The colors represent amount of spread over a specific period. Map courtesy of Fire progression map courtesy USDA Forest Service-Superior National Forest
Figure 3: Traces of daily HDW values for a 29-day period centered on the largest spread day for Bastrop (a) and La Brea (b) wildland fire events. Red dates and shading represent reported fire dates. Black line signifies the largest fire spread day
Figure 4: HDW values for all meteorological datasets and wildland fire events during a 29-day period centered on the largest fire spread day. The black line separates western fire events from central and eastern fire events
Figure 5: HDW values for all meteorological datasets and wildland fire events during a 11-day period centered on the largest fire spread day. The black line separates western fire events from central and eastern fire events
Figure 6: HDW skill for all of the meteorological analysis datasets and wildland fire events. White boxes indicate HDW success, and colored boxes indicate unsuccess. Hit rates are also provided
Figure 7: The expansion of the plots presented in Fig. 6 to include the eight grid points surround the central grid point
Figure 8: Same as Fig. 6 but for an HDW formulation using a 1500-m deep layer34
Figure 9: Same as Fig. 6 but for an HDW formulation using a 1000-m deep layer34
Figure 10:The expansion of the plots presented in Fig. 8 to include the eight grid points surround the central grid point
Figure 11: The expansion of the plots presented in Fig. 9 to include the eight grid points surround the central grid point
Figure 12: Same as Fig. 6 but for an HDW formulation using all available analysis dataset hours between 1200 UTC and 0000 UTC
Figure 13: Same as Fig. 6 but for an HDW formulation using all available analysis dataset hours between 1200 UTC and 0600 UTC

Figure 14: Same as Fig. 6 but for an HDW formulation using 1200, 1800, 0000 and 0600 UTC 39
Figure 15: The expansion of the plots presented in Fig. 12 to include the eight grid points surround the central grid point
Figure 16: The expansion of the plots presented in Fig. 14 to include the eight grid points surround the central grid point
Figure 17: Same as Fig. 6 but for an HDW formulation using a 1000-m deep layer and 1200, 1800, and 0000 UTC
Figure 18: Same as Fig. 6 but for an HDW formulation using a 1000-m deep layer and 1200, 1800, 0000 and 0600 UTC
Figure 19: Same as Fig. 6 but for an HDW formulation using a 1500-m deep layer and 1200, 1800, 0000 UTC
Figure 20: Same as Fig. 6 but for an HDW formulation using a 1500-m deep layer and 1200, 1800, 0000 and 0600 UTC
Figure 21: Same as Fig. 6 but for an HDW formulation using a 1000-m deep layer and all available analysis dataset hours between 1200 and 0600 UTC
Figure 22: Same as Fig. 6 but for an HDW formulation using a 1500-m deep layer and all available analysis dataset hours between 1200 and 0600 UTC
Figure 23: The expansion of the plots presented in Fig. 18 to include the eight grid points surround the central grid point
Figure 24: The expansion of the plots presented in Fig. 19 to include the eight grid points surround the central grid point
Figure 25: The expansion of the plots presented in Fig. 20 to include the eight grid points surround the central grid point
Figure 26: The expansion of the plots presented in Fig. 21 to include the eight grid points surround the central grid point
Figure 27: The expansion of the plots presented in Fig. 22 to include the eight grid points surround the central grid point
Figure 28: The expansion of the plots presented in Fig. 23 to include the eight grid points surround the central grid point

KEY TO ABBREVIATIONS

AGL – Above Ground Level
ANT – Antelope
BAS – Bastrop
BMD – Big Meadows
BRF – Black River Falls
BRG – Bridger
BUG – Bugaboo
CFFDRS – Canadian Forest Fire Danger Rating System
CFSR – Climate Forecast Reanalysis
CONUS – Continental United States
ESR – East Slide Rock Ridge
F – A Simple Fire Danger Index
FFWI – Fosberg Fire Weather Index
FWI – Fire Weather Index

GFS – Global Forecast System

HDW - Hot-Dry-Windy Index HI – Haines Index HLK - Ham Lake HS2 – Horseshoe 2 IJWF – International Journal of Wildland Fire IMET – Incident Meteorologist LAB – La Brea LON-LonesomeLOS – Los Conchas MIF - Milford Flat MON – Monument MUR - MurphyMUS - Mustang Corner MWC - Matador West NAM – North American Meso-Scale Model NARR – North American Regional Reanalysis

NFDRS - National Fire Danger Rating System

PCR – Pagami Creek

RH – Relative Humidity

RUC – Rapid Update Cycle Model

SCZ-Schultz

STA – Station

TMB-Tumble bug

UTC -Universal Time Coordinated

VPD – Vapor Pressure Deficit

WAL-Wallow

WCR - Witch Creek

CHAPTER I – INTRODUCTION

In the last three decades, an increase in wildland fire frequency, severity, and in length of the fire season has been observed (Abatzoglou and Kolden 2013). Three examples are the High Park Fire of 2012 in Colorado that burned 87,000 acres, destroyed 259 homes, killed one person, and cost \$38 million to suppress (Gabert 2015); the California Wine Country fire events that burned more than 110,000 acres in October, 2017 and destroyed approximately 7,000 structures (California Department of Forestry 2017); and the Carr Fire in California of 2018 that burned 229,651 acres, destroyed 1,604 structures, and was the 6th most destructive fire in California's History (CNN WIRE 2018, CA.gov 2019). Recent studies suggest this increase in fire activity and the lengthening of fire seasons will continue in coming years (McKenzie et al. 2004). These anticipated increases highlight the importance of the ability to predict when a fire could be more dangerous in order to prevent loss of life and property, and to improve wildland fire management strategies.

Fire-weather forecasters, incident meteorologists (IMETs), and fire managers use fire-danger rating systems, fire-behavior analyses, and fire-weather tools to assess the potential for wildland fire events to threaten lives and property. Fire indices are a common component in these fire environment products. A fire index relays information on the potential for environmental conditions to contribute to one or more characteristics of a wildland fire. Different types of fire indices provide information on variables such as fuels, spread rates, energy release rates, and weather. Some of the indices combine multiple types of variables, while others are specific to one type. There are many fire indices and systems of indices currently in use around the world. For example, the National Fire Danger Rating System (NFDRS) (Schlobohm and

Brian 2002) is a system that uses a collection of indices and components to help inform staffing levels, preparedness levels, and fire adjective ratings to fire managers in the United States.

Analogous systems are used in Canada (the Canadian Forest Fire Danger Rating System,

CFFDRS, Van Wagner 1974) and Australia (the McArthur Fire Danger Rating System,

McArthur 1966, 1967). Examples of stand-alone indices include the Lower Atmospheric

Stability Index, also known as the Haines Index (HI) (Haines 1988), Angström Index (Langholz et al. 1993), Sharples Index (Sharples et al. 2009), and the index developed by Erickson et al. (2016).

Although these systems and indices provide important fire information, they are often misused due to the lack of investigational studies to validate their implementation. For example, rigorous studies of the NFDRS to validate the use of each component or to relate the outputs to decision-making strategies have not been conducted. The NFDRS also accounts for weather parameters more than once, artificially inflating the influence of those variables on the outputs provided by the system. Another example is the HI, which does not account for wind but would be improved upon the addition of a wind component (Potter 2018). Two studies have been published on the HI to validate its use and skill in predicting wildland fire behavior (Werth and Ochoa 1993, McCaw et al. 2007). To improve on the information that is currently available to fire-weather forecasters, IMETs, and fire managers, new indices have been developed that require validation to establish their usefulness to avoid misinterpretation.

To address the shortcomings of current systems and indices, a new fire-weather index called the Hot-Dry-Windy Index has been developed to diagnose the potential for atmospheric conditions in the vicinity of a fire to affect the evolution of that fire. HDW considers only meteorological variables in its formulation, differentiating it from other indices that include fuel

and topography information. The development of this index was aided by the recent establishment of long-term reanalysis datasets (Srock et al. 2015) and tested using the Climate Forest System Reanalysis (CFSR, Saha et al. 2010) on four historical wildland fire events: Pagami Creek Fire of 2011, Bastrop Fire of 2011, Double Trouble Fire of 2002, and the Cedar Fire of 2003 (Srock et al. 2018). McDonald et al. (2018) further develops HDW by creating a 30-year climatology of the index and uses the climatology to establish percentiles to aid in the interpretation of HDW values and traces calculated using the Global Forecast System (GFS, Wei 2008) dataset.

While two previous studies develop HDW and show how the index works as a forecast product, further investigation using additional meteorological datasets and wildland fire events is needed prior to the implementation of the index into operational fire-weather forecasts. This study analyzes HDW using five meteorological analysis datasets for twenty-three historical wildland fire events. A meteorological analysis dataset in the context of this study refers to a dataset that starts with a meteorological model as a first guess and then assimilates observations from multiple sources to produce a gridded analysis of meteorological conditions for the CONUS. An analysis dataset can be either a reanalysis or grids from the analysis times of a forecast model. Note that although analyses from forecast models are used in this study, no forecast data is used. The HDW values produced using each analysis dataset are evaluated and differences between the values for each dataset and between fire events are explained. Additionally, the sensitivity of HDW values to the assumptions made in its development are investigated to optimize the formulation of the index. The objective of this study is to provide information to fire-weather forecasters, IMETs, and fire managers that will facilitate the interpretation of HDW, in turn helping them implement the index operationally.

The rest of the thesis is organized following the 'paper format'. Chapter II provides a literature review of fire danger rating systems and fire indices; Chapter III consists of a full article to be submitted to International Journal of Wildland Fire (IJWF), which includes an introduction with background information, detailed description of the method used, and discussion of the analysis results; Chapter IV extended results and conclusion; Chapter V presents supplementary results and discussion; Bibliography.

CHAPTER II – LITERATURE REVIEW

In this chapter, descriptions of fire danger rating systems and fire indices are provided.

The necessary inputs to the systems or indices and how the outputs are commonly used are discussed to provide background on the differences between the systems and indices, and to provide conceptual understanding on the different types of systems and indices in use today.

1. Fire Weather Systems and Indices

1.1 Fire Danger Rating Systems

A fire danger rating system is a system employing the use of multiple indices to provide information to fire managers, which is used to determine levels of fire preparedness. One such system is the National Fire Danger Rating System (NFDRS). The NFDRS was first released in 1972, and in 1975 the automated version of the NFDRS was released. The most recent update to the NFDRS occurred in 2001. The hourly meteorological inputs to this system are wind speed, relative humidity, temperature, solar radiation, and rainfall, of which go into calculating the 1-hour, 10-hour, 100-hour, and 1000-hour fuel moisture. The daily meteorological inputs are vapor pressure deficit, minimum temperature, day length, maximum temperature, and rainfall, that produce the live herbaceous and woody fuel moisture, and the Keetch-Byram Drought Index. The fuel moistures and drought index go into the production of the ignition component, spread component, burning index, and energy release component. The last three components are combined to establish the staffing level index, staffing level, and adjective fire danger rating (National Wildfire Coordinating Group, 2002).

The Canadian Forest Fire Danger Rating System (CFFDRS, Van Wagner 1974) is a system that was developed in the 1920's to inform users of how the environment is impacting the

fire danger and fire behavior of a wildland fire (National Wildfire Coordinating Group, 2017). The system's inputs are risks of a wildland fire being initiated, weather, topography, and fuels. From these inputs, the fire occurrence prediction system, fire weather index system, accessory fuel moisture system, and fire behavior prediction system are filled and combined to guide fire management decision and to aid fire research in developing solutions.

1.2 Fire Indices

A fire index is a tool using combinations of variables such as fuel, topography, and weather to define a relationship between these combinations and wildland fire events. Several fire indices have been developed and are continuing to be developed to aid in managing fire events and providing information about relationships between fire events and the environments surrounding a fire. Examples of indices described in this chapter include the Angström Index (Langholz and Schmidtmayer 1993, Willis et al. 2001), the Fosberg Fire Weather Index (Fosberg 1974), the Haines Index (Haines 1978), an index developed by Sharples et al. (2008), the modified Fosberg Fire Weather Index (Goodrick 2002), the Fire Weather Index (Erickson et al. 2015), and the recently developed Hot-Dry-Windy Index (Srock et al. 2018).

The Angström Index provides a once-daily assessment of heat and moisture by comparing observed values of temperature and relative humidity to reference values. The index is used to provide asses the favorability of fire conditions for the day. It is used as both a standalone index and part of a forecast tool. Nunes et al. (2017) investigated how this index performed as a stand-alone index in Brazil for the years from 2012 through 2015. The results of this study conclude that this index correctly identified the fire season and that this index was a useful tool to aid in planning wildland fire fighting strategies for Brazil.

An index used to assess fire danger ratings for bushfire occurrences is created in Sharples et al. (2008). The index proposed in this article (F) is developed and compared with fire danger indices produced by fire danger rating systems that establish fuel conditions. F is designed to be simple in calculation and intuitive in application. The index is calculated using the wind and the fuel moisture content provided by a fire danger rating system. Sharples et al. (2008) compared F with four alternative fire indices and found a significant correlation between F and the alternative indices. No further studies exist that evaluate the performance of this index with actual fire events.

Fosberg (1974) creates a fire-weather index that is referred to as the Fosberg Fire Weather Index (FFWI). This index is developed to provide information on how weather impacts fine fuels and how those fuels impact a fire. The FFWI is meant to be a supplement to fire danger calculations for higher resolution information on these impacts. To calculate this index, the forward rate of spread is determined by the windspeed and the fuel moisture content is determined by the relative humidity and temperature. The intended use of the FFWI is to provide hourly and bihourly weather information using maps to show the spatial and temporal variations in the weather. The index is also intended to establish the progression rate of the diurnal fluctuations in fire weather. The FFWI has been validated using one fire event and two days of surface observations. This index is designed to only be used for the NFDRS and is not intended to be a stand-alone index.

A study of the FFWI is conducted by Goodrick (2002) to assess the impact of precipitation on the index. It uses the Keetch-Byram Drought Index to provide information on fuel availability to enhance the FFWI performance. Breakpoints for the FFWI are established based on values of the modified index (mFFWI) observed from January 1981 through June 2001

for 120 National Weather Service observational sites in Florida. The result of this study shows that the mFFWI is more skillful in measuring a fire's potential and the impact of dry versus wet cold frontal passage on this potential. There have been no rigorous studies in the mFFWI in other regions of the US.

Erickson et al. (2015) develops a statistical weather-based fire index (FWI) for a subregion of the Northeastern United States using fire occurrence data from 1999 to 2008. This index is designed to predict wildfire occurrence using only atmospheric variables. Climatological average of meteorological variables collected from Automated Surface Observing Systems (ASOS) are compared with wildfire occurrence data to statistically establish the impact of specific variables on wildland fire occurrence. This study found that the temperature and relative humidity are to main two meteorological variables with the largest statistical sign of prediction of wildfire occurrences. To define the FWI, relative humidity and temperature are employed in a binomial logistic regression, and the FWI is shown to have more probabilistic skill than climatology. Further testing of the FWI to establish its ability to forecast fire occurrence using gridded meteorological analysis datasets is suggested. Although the FWI is investigated using ensemble numerical weather prediction data (Erickson et al. 2018), no studies of the performance of this index in predicting wildland fire occurrences have been conducted.

The Haines Index (HI) is intended to communicate the potential for fire to become large or erratic (Haines, 1988). The HI is defined using the lapse rate between two atmospheric levels, and the dewpoint depression at a single level. These values are binned individually from one to three based on their magnitude and these two bins are then summed to produce the index value. There are three variants of the Haines Index based on low, mid, and high elevations. The low elevation considers the lapse rate from 950 hPa to 850 hPa and the dewpoint depression at 950

hPa. The mid elevation's lapse rate term is from 850 hPa to 700 hPa and its dewpoint depression is at 850 hPa. The high elevation's lapse rate is from 700 hPa to 500 hPa, while the dewpoint depression is collected from at 700 hPa. This index cannot have a value less than two or greater than six.

Werth and Ochoa (1993) investigates the HI to establish the difference in validity of the index for "plume-dominated" fire events and "wind-driven" fire events. The study uses two fire events in Idaho from 1988 and 1989. They establish the 1988 wildland fire was "plume-dominated", and that the HI identified when the fire activity was more dangerous. The 1989 wildland fire was "wind-driven", and the HI is found to be incapable of identifying when the fire activity was more dangerous. McCaw et al. 2007 evaluates a climatology of the index using four bushfire events in southwestern Australia. This study found that HI values are most often 6 for December and January (summer) in southwestern Australia, and that values of 5 or 6 are associated with higher values of the McArthur Grassland Fire Danger Index (GFDI, McArthur 1966). The correlation of high HI values with high GFDI values are an indication that days with significant fire spread potential are identified by the current fire danger rating system used in Australia.

HDW is developed to assist fire-weather forecasters with predicting when synoptic-and meso-alpha-scale weather conditions will make a wildland fire difficult to manage (Srock et al 2018. The index is presented as a tool to assess "how the atmosphere can affect a fire" and to diagnose the potential for atmospheric conditions to contribute to more dangerous fire behavior. The index is calculated by multiplying the maximum vapor pressure deficit (VPD) [hPa] and the maximum windspeed [m/s] in a layer extending 500-m from the Earth's surface. HDW uses VPD instead of relative humidity (RH) because VPD is correlated with fuel evaporation rates,

and therefore can quantify the potential for both temperature and moisture to impact a wildland fire.

Srock et al. (2018) uses four historical wildland fire events (Pagami Creek (MN), Bastrop County Complex (TX), Double Trouble (NJ), and Cedar (CA)) to assess the performance of HDW using the CFSR dataset. These historical wildland fire events are chosen because they provide different types of topographic environments for which HDW could be analyzed. A comparison of HDW with HI shows that HDW out-performed HI for this selection of historical wildland fire events. The results from this study show that HDW can identify the day during a fire on which the wildland fire's behavior was most dangerous and therefore the most difficult to manage.

McDonald et al. (2018) produced a 30-year HDW climatology using CFSR to provide users with information about the daily and seasonal variability of the index. To aid in the interpretation of HDW, percentiles from this climatology are computed to identify when anomalous HDW values occurred. When the percentiles are used with daily traces of HDW values from a forecast model (GFS, Wei 2008), users can evaluate trends in HDW and compare those trends with historical values. The GFS is selected because it has the same temporal resolution and horizontal grid spacing as the CFSR. This study found that the percentiles signified anomalously high HDW values in the traces of the historical wildland fire events and shows that the percentiles aid in the interpretation of specific HDW values for multiple locations in the United States.

2. Summary

The NFDRS and CFFDRS, the Angström Index, F, FFWI, FWI, HI, and HDW are described in this section. These indices are examples of fire-weather indices and indices that

combine weather and fuel variables in their calculations. Of the two fire danger rating systems and the six fire indices described in this study, only HI and HDW have studies published to validate or interpret index values and their relation to fire behavior. The studies on the HI conclude that there are deficiencies in its calculation, and that an alternative formulation is more useful in Australia. Further investigations of the HI to include winds into the formulation to improve its skill are suggested by Potter (2018).

None of these indices have been rigorously validated with fire data to establish their validity as fire-weather indices, which weakens arguments pertaining to their use in systems of indices and as stand-alone indices as they have not been proven to be skillful in providing their intended information. Although previous HDW studies demonstrate the potential of the index to identify the dangerous fire behavior day, they are limited to four fire events and one analysis dataset. The current study will expand on the validation of HDW using a larger number of fire events and datasets.

CHAPTER III – AN EVALUATION OF THE HOT-DRY-WINDY FIRE-WEATHER INDEX USING HISTORICAL FIRE EVENTS AND METEOROLOGICAL ANALYSIS DATASETS

1. Introduction

As wildland fire activity and severity increases (Abatzoglou JT, Kolden CA, 2013), the tools used to prevent loss of life and property, and to improve wildland fire management strategies become more important. These tools include fire indices and system of indices that provide information on the potential for environmental factors to impact a fire. Some examples of these tools are the National Fire Danger Rating System (NFDRS, Schlobohm and Brian 2002), the Canadian Forest Fire Danger Rating System (CFFDRS, Van Wagner 1974), the McArthur Fire Danger Rating System (McArthur 1966, 1967), the Lower Atmospheric Stability Index, also referred to as the Haines Index (HI, Haines 1988), the Angström Index (Langholz H. and E. Schmidtmayer 1993, Willis et al. 2001), the Sharples Index (Sharples et al. 2009), and the index developed by Erickson et al. (2016). These tools are often misused due to a lack of investigational studies validating their purpose and ability to represent specific relationships to wildland fire activity. New indices are being and have been developed recently to address the shortcomings of the indices currently is use today.

To address the shortcomings of current systems and indices, the development of a new fire-weather index called the Hot-Dry-Windy Index (HDW, Srock et al. 2018) has been undertaken. HDW is designed to indicate the potential for the weather to affect a wildland fire using meteorological variables that can be predicted by operational numerical weather prediction models at synoptic- and meso-alpha scales. This index is defined as the product of the maximum

vapor pressure deficit (VPD) and the maximum windspeed found in the lowest 500 m of the atmosphere. A daily value of HDW for application in the continental United States (CONUS) is determined by calculating the index value at 1200, 1800, and 0000 UTC (the next day) and identifying the maximum value for those three times. Srock et. al. (2018) uses the Climate Forecast System Reanalysis (CFSR, Saha et al.2010) to show that HDW identified the day on which the most dangerous fire behavior was reported during four historical wildland fire events in the CONUS. The study concluded that further validation of HDW is necessary to establish the skill and usefulness of this index for the fire community. It is also recommended that alternative formulations of HDW using different analysis layers on finer temporal and spatial scales be investigated.

McDonald et al. (2018) conducted a second study that produced a 30-year climatology of HDW using the CFSR showing the daily and seasonal variability of the index. The Global Forecast System (GFS, Wei et al. 2008) is used to produce traces of daily HDW values during four historical wildland fire events and those traces are compared with the climatology to identify anomalous values of HDW and assess their significance. This study established that the CFSR climatology and GFS forecast traces can be used to "produce a single product that provides seasonal, climatological, and short-term context to help determine the appropriate firemanagement response to a given HDW value." McDonald et. al (2018) suggested that further studies using more wildland fire events with additional forecast models should be conducted to show the variance of HDW's skill.

For this study, two HDW investigations are undertaken in response to the recommendations in Srock et al. (2018) and McDonald et al. (2018), and to establish the skill of the index as it is intended to be used. First, an inter-comparison of HDW values derived from

additional meteorological analysis datasets and historical wildland fire events will be conducted. Second, the sensitivity of HDW values to the assumptions made in its development are investigated. Alternative formulations are evaluated to determine differences in skill at capturing conditions conducive to extreme behavior on existing fire events. One reanalysis dataset and two forecast model analyses are used in addition to the CFSR and GFS used in Srock et al. (2018) and McDonald et al. (2018).

The following section describes the meteorological analysis datasets, the wildland fire events, and the methodology for assessing the skill of HDW for the fire events. Section 3 presents the results of this assessment, and section 4 discusses the implications of the results, presents conclusions, and proposes future work.

2. Data and Methods

2.1 Meteorological Analysis Datasets

A meteorological analysis dataset, in the context of this study, refers to a dataset that starts with a meteorological model as a first guess and then assimilates observations from multiple sources to produce a gridded analysis of meteorological conditions for the CONUS. An analysis dataset can be either a reanalysis or it can be grids from the analysis times of a forecast model. Note that although analyses from forecast models (described below) are used in this study, no forecast data is used to evaluate HDW. All of the characteristics of the analysis datasets described below are based on the version of the datasets available in archives.

In addition to the reanalysis dataset used in Srock et al. (2018) and McDonald et al. (2018) (CFSR), this study uses data from the North American Regional Reanalysis (NARR, Messinger et al. 2005). The CFSR dataset has a horizontal grid spacing of ~56 km (0.5° latitude), 29 available vertical pressure levels, and a 6-hour temporal resolution. The lowest pressure level

is 1000 hPa and the highest is 50 hPa. The CFSR also provides temperature at 2 m above ground level (AGL) and wind at 10 m AGL. The NARR dataset has a horizontal grid spacing of 32 km, and a 6-hour temporal resolution. There are 29 vertical pressure levels available in the NARR and the lowest pressure level is 1000 hPa while the highest is 100 hPa. The NARR also provides 2 m AGL temperature and wind data from 10 m up to 30 m AGL.

In addition to the forecast dataset used in McDonald et al. (2018) (GFS), this study uses forecast model analyses from the North American Mesoscale Forecast System (NAM, Janic Z. 1997) and the Rapid Update Cycle (RUC, Benjamin et al. 2004). The GFS analyses, like the CFSR, have a horizontal grid spacing of ~53 km, and a 6-hour temporal resolution. There are 26 vertical pressure levels, and the lowest pressure level is 1000 hPa while the highest is 10 hPa. The GFS, and the rest of the forecast model analyses used in this study, also provide 2 m AGL temperature data and 10 m AGL wind data. The NAM has a horizontal grid spacing of 12 km, and a 6-hour temporal resolution. There are 29 vertical pressure levels, and the lowest pressure level in the NAM is 1000 hPa while the highest is 100 hPa. The RUC has a horizontal grid spacing of 12 km, and 1-hour temporal resolution. There are 37 vertical pressure levels, and the lowest pressure level is 1000 hPa while the highest is 100 hPa.

The archive data this study uses is downloaded from two sources. The preferred source being the National Operational Model Archive and Distribution System (NOMADS) data archive provided by the National Oceanic and Atmospheric Association (NOAA) because of the ease of access. The secondary source is the NCAR research data archive (RDA; http://rda.ucar.edu/datasets/ds335.0/). Data is collected for a 29-day period centered on the largest fire spread day (the methodology of determining this day is discussed in the section 2.3) for each wildland fire event used in this study. The name, abbreviation, horizontal grid spacing,

temporal resolution, and the number of vertical levels for the meteorological analysis datasets used in this study are listed in Table 1.

Table 1: Information for the five meteorological analysis datasets used in this study. Their names, abbreviations, and spatial and temporal resolutions are provided

Meteorological Analysis Dataset	Dataset Abbreviation	Horizontal Grid Spacing	Temporal Resolution	Number of Vertical Pressure Levels
Climate Forecast System Reanalysis	CFSR	~ 53 km	6-hour	29
Global Forecast System	GFS	~ 53 km	6-hour	26
North American Regional Reanalysis	NARR	32 km	3-hour	29
Rapid Update Cycle	RUC	20 km	1-hour	37
North American Mesoscale Forecast	NAM	12 km	6-hour	29

2.2 Wildland Fire Events

The twenty-three wildland fire events selected for this study are chosen to provide geographic diversity. By choosing wildland fire events that occur in diverse terrain and regional climates, the ability of HDW to capture conditions conducive to extreme fire behavior for a range of fire environments can be investigated. Of the twenty-three fire events, two occurred in the Eastern United States (US), six occurred in the Central US, and 15 occurred in the Western US. There are fewer Eastern US wildland fire events because this study requires multi-day events with a single extreme day for which archives of all the meteorological analysis datasets are available. Events with these characteristics are uncommon in the eastern US. HDW is designed to identify days when a wildland fire could be difficult to manage, and wildland fire events are more difficult to manage when extreme fire behavior occurs. According to Werth et al. (2017), extreme fire behavior is defined as "Fire spread other than steady surface spread, especially when it involves rapid increases". The wildland fire events selected for this study have spread data that allows the day when the most spread occurred to be determined. For

these twenty-three events, it is not possible differentiate between days on which rapid fire spread occurred and days exhibiting steady surface spread. However, the day on which the most fire spread occurred should have a greater potential for extreme fire behavior than other days on the fire event.

The locations of the wildland fire events are presented in Fig. 1, and Table 2 lists the names, locations, latitudes, longitudes, and the day identified to have the largest fire spread for each fire event are provided. These fire events are chosen because they provide geographic diversity, they occurred within the temporal range of the available meteorological datasets because of the availability to information on their spread characteristics. Twenty-three fire events are chosen to provide enough data for statistical analysis of HDW's skill.

Table 2: The names, abbreviations, locations, elevations, latitudes, longitudes, and date of largest fire spread of the twenty-three wildland fire events are provided

Wildland Fire (Abbrev.)	Location	Elevation [m]	Latitude	Longitude	Date of Largest Spread
Antelope (ANT)	California	4,059	40.0	-119.7	07/05/2007
Bastrop County (BAS)	Texas	51	30.1	-97.3	09/04/2011
Big Meadows (BMD)	California	1,501	40.3	-105.7	08/27/2009
Black River Falls (BRF)	Michigan	506	46.5	-87.4	05/20/2009
Bridger (BRG)	Colorado	1,869	37.4	-87.0	06/11/2008
Bugaboo (BUG)	Florida	54	31.1	-82.5	05/10/2007
East Slide Rock Ridge (ESR)	Nevada	2,573	41.1	-115.3	08/25/2008
Ham Lake (HLK)	Minnesota	600	45.2	-93.2	05/10/2007
Horseshoe 2 (HS2)	Arizona	1,513	31.8	-109.2	05/09/2011
La Brea (LAB)	California	14	34.9	-119.9	08/13/2009
Lonesome (LON)	Oregon	2,077	42.0	-123.9	09/18/2008
Los Conchas (LOS)	New Mexico	1,475	35.8	-106.2	06/26/2011
Matador West (MWC)	Texas	829	34.0	-100.8	02/27/2011
Milford Flat (MIF)	Utah	1,747	38.3	-113.0	07/07/2007
Monument (MON)	Arizona	3,053	31.5	-110.2	06/19/2011
Murphy (MUR)	Nevada	2,003	42.5	-116.1	07/18/2007
Mustang Corner (MUS)	Florida	2	25.4	-80.5	05/15/2008
Pagami Creek (PCR)	Minnesota	616	47.8	-91.3	09/12/2011
Schultz (SCZ)	Arizona	2,743	34.9	-111.5	06/21/2010
Station (STA)	California	43	33.9	-118.3	08/30/2009
Tumblebug (TMB)	Oregon	1,530	43.4	-122.2	09/21/2009
Wallow (WAL)	New Mexico	1,840	33.6	-109.4	06/06/2011
Witch Creek (WCR)	California	1,068	32.7	-117.1	10/22/2007

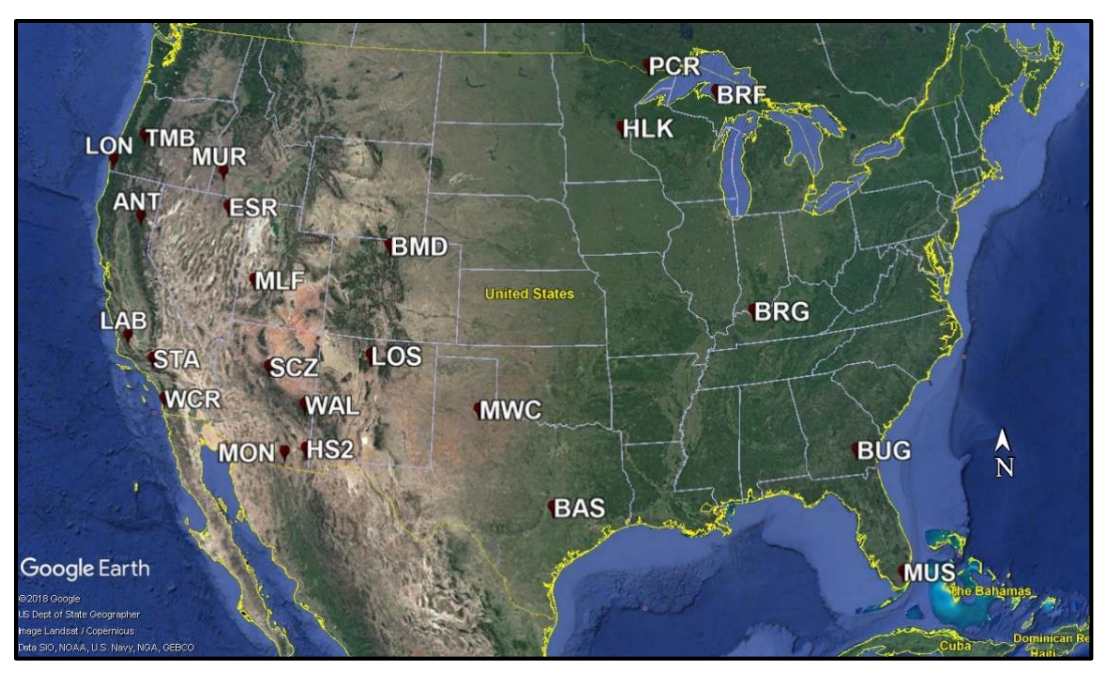


Figure 1: Map presenting the locations of the twenty-three historical wildland fire events created using Google Earth Pro

2.3 Selecting the Largest Fire Spread Day

Fire spread maps (e.g. Fig. 2 for the La Brea Fire) are used, when available, to identify the largest spread day for each fire. When a fire spread map was unavailable, literature on a given fire case helped to identify the day the largest spread occurred. For instance, a fire behavior report on the lessons learned during a fire or a National Interagency Fire Center report often indicates the largest fire spread day. When no spread map or report was available, members of the fire community are consulted to establish the largest fire spread day for those fire events.

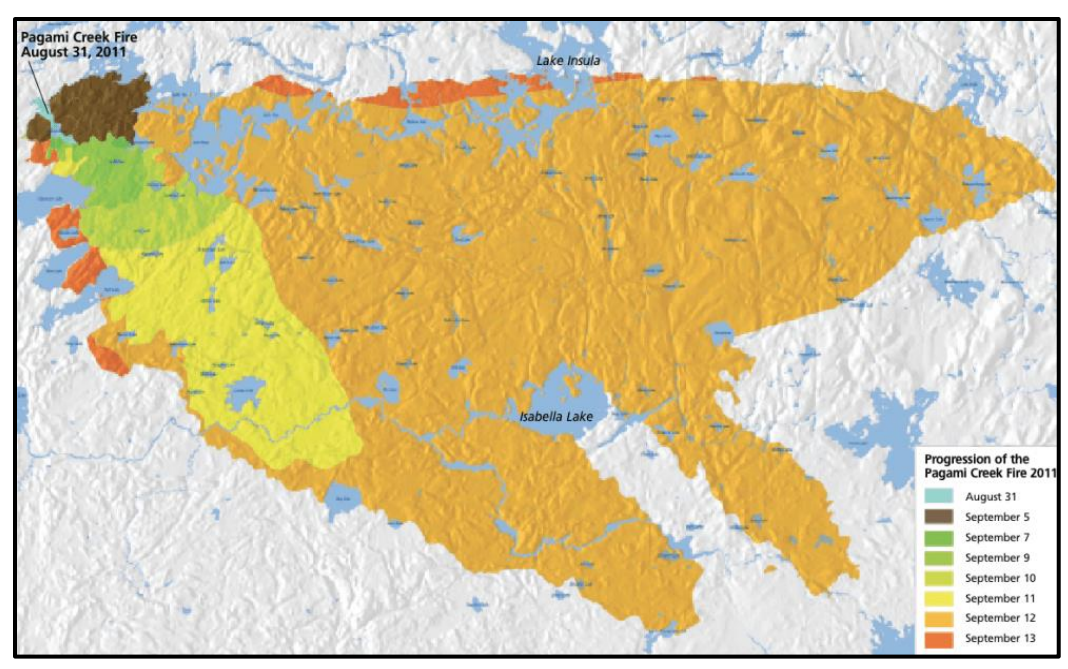


Figure 2: A fire progression map for Pagami Creek fire event. The colors represent amount of spread over a specific period. Map courtesy of Fire progression map courtesy USDA Forest Service-Superior National Forest

2.4 Evaluating HDW Skill

Characteristics of fire data can vary depending on the source and depending the method of data collecting and reporting. According to Potter (2008), fire spread data can be reported differently for the same fire, and there are circumstances when a fire's reported largest spread day can differ from the actual largest spread day by up to two days depending on the data source. To address this uncertainty, HDW's skill is evaluated for each analysis dataset and wildland fire event. During an 11-day period centered on the largest spread day, the HDW value at the grid point containing the latitude and longitude of the fire event is analyzed to determine if it maximized on the day of or one day prior to the largest spread day. Only the days on which a fire was reported are considered for these evaluations. When HDW maximized on the day of or the day before the largest fire spread day, the index is considered a success for that fire event and analysis dataset. The rate of success is determined by dividing the number of successes by the total number of fire events. When HDW is not successful at identifying the maximum spread

day, the difference between the day when HDW maximized and the largest spread day is also recorded.

3. Sensitivity Testing

In the original formulation presented in Srock et al. (2018), the hours of 1200, 1800, and 0000 UTC are used because of the temporal resolution of their dataset. With the addition of analysis datasets containing higher temporal resolutions, investigation into the sensitivity of the original HDW formulation can be conducted. This is done by comparing the original formulation with the maximum available temporal resolution of each analysis dataset for all times available between 1200 UTC and 0000 UTC. The archived analyses of the CFSR, GFS, and NAM have 6-hourly temporal resolution, the NARR is 3-hourly, and the RUC is hourly.

In addition to using times between 1200 UTC and 0000 UTC, the impact of using additional times through 0600 UTC is investigated. HDW is originally calculated using 1200, 1800, and 0000 UTC because Srock et al. (2018) argued that it encompassed the burn period for a day. However, the impact of extending the period to 0600 UTC has not been investigated. This study tests how sensitive HDW is to the original times by comparing them to HDW calculations with the addition of 0600 UTC. Further testing of this sensitivity will be conducted to include all available analysis dataset temporal values from 1200 UTC to 0600 UTC to evaluate if the higher temporal resolution datasets yields higher skill.

A 500-m deep layer is chosen by Srock et al. (2018) to account for the weather conditions that are most likely to interact with a wildland fire during a burning period, and it is unclear how sensitive HDW values are to this choice. To test this sensitivity, HDW is first calculated using a layer depth of 500 m from the original formulation and compared to HDW values calculated using a layer depth of 1000 m and 1500 m. To account for differences in vertical grid spacing

between the analysis datasets, the layer begins at the surface and extends to the first pressure level with a height greater than or equal to the layer depth being tested.

4. Results

4.1 Distributions of HDW Values

Examples of 29-day HDW time series centered on the largest fire spread day are shown for the five analysis datasets on the Bastrop (Fig. 3a) and the La Brea (Fig. 3b) fire events. The dates colored in red indicate the days when the fire events were reported. There is a daily variation amongst HDW values, ranging from approximately 100 to 700. The amplitude distributions of HDW for Bastrop reveal larger synoptic variations and larger magnitudes of index values than for La Brea. There appears to be three synoptic cycles associated with Bastrop, however for La Brea synoptic cycles are less clear. The analysis datasets show a peak in magnitude of HDW values on the largest spread day for Bastrop, while for La Brea the largest spread day does not exhibit the highest HDW value for all of the analysis datasets. The difference in analysis dataset agreement for these two wildland fire events could be attributed to differences in orography, surface characteristics, and spatial resolution of the datasets.

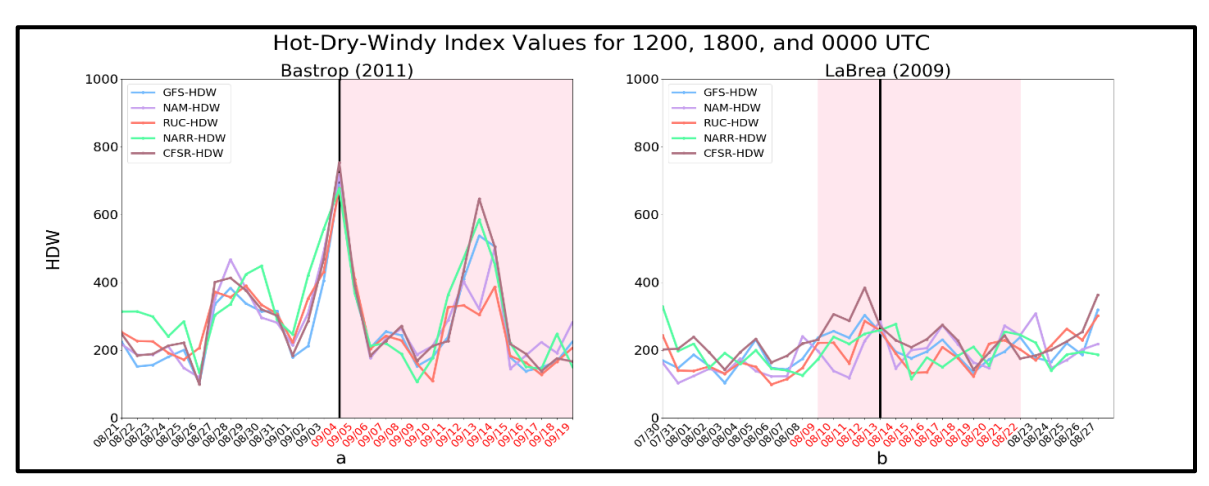


Figure 3: Traces of daily HDW values for a 29-day period centered on the largest spread day for Bastrop (a) and La Brea (b) wildland fire events. Red dates and shading represent reported fire dates. Black line signifies the largest fire spread day

To show HDW values for a range of synoptic conditions, the distributions of index values for a 29-day period centered on the largest spread day for each fire and all meteorological analysis datasets are shown in box and whisker plots (Fig. 4). The fire events are ordered from left to right based on longitude, with the western-most event appearing on the left. The vertical black line plotted between Bridger (BRG) and Matador West Complex (MWC) represents the beginning of central and eastern fire events. In this analysis, the highest over-all HDW values and largest range of values occurred on the Lonesome Complex (LON), whereas the smallest ranges of HDW values occur for the Antelope (ANT) and Mustang Corner (MUS) fire events. Although the ranges in HDW values produced by each analysis dataset for each fire exhibit unique characteristics, no specific analysis dataset appears to be an outlier for any of the fire events. Based on the 29-day analyses, no clear west-to-east pattern is apparent in the range of HDW values on these fire events, and no analysis dataset is found to differ substantially from the other datasets for a majority of the events.

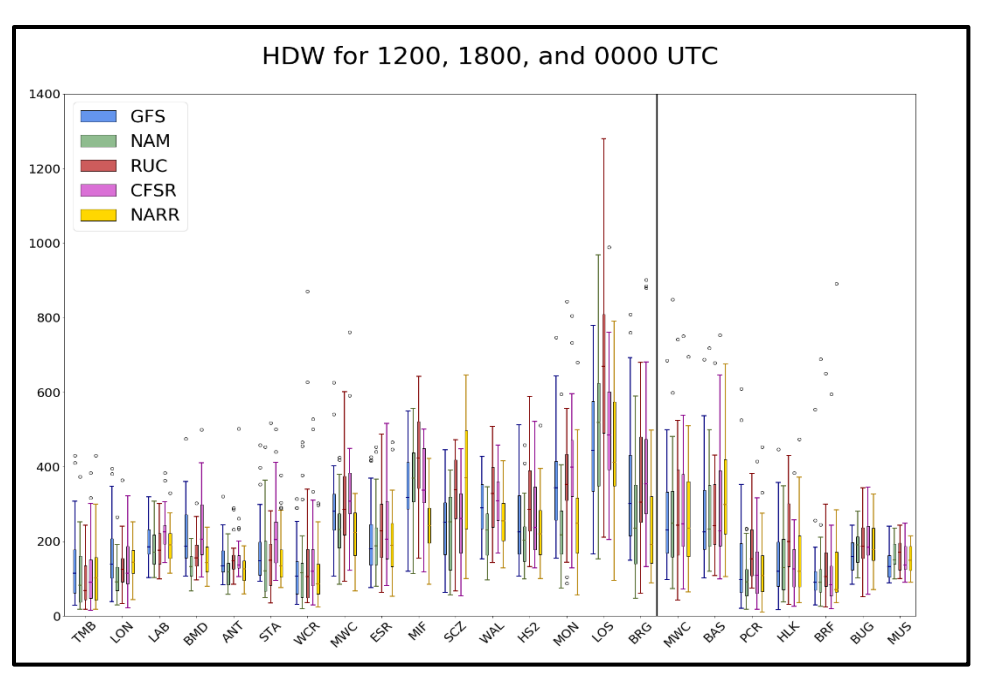


Figure 4: HDW values for all meteorological datasets and wildland fire events during a 29-day period centered on the largest fire spread day. The black line separates western fire events from central and eastern fire events

4.2 Analysis Dataset Skill Comparisons

The rest of the analyses in this study will focus on an 11-day period centered on the largest fire spread because HDW is designed to predict the synoptic- and meso-alpha scale weather conditions conducive to dangerous fire behavior. Figure 5 shows box and whisker plots of the 11-day HDW values for all twenty-three wildland fire events and for the five meteorological analysis datasets used. Note that only the days on which fire was reported are represented in this plot. As with the 29-day analysis (Fig. 4), there is still no analysis dataset that differs substantially for all the fire events. However, the 11-day analyses exhibit larger differences in range between the analysis datasets for individual events (e.g. BMD, LON, and MWC). Due to the reduction from 29 to 11 days, values previously marked as outliers in Fig. 4 now appear as whiskers in Fig. 5. These 11-day HDW values are used in the rest of the analyses in this study.

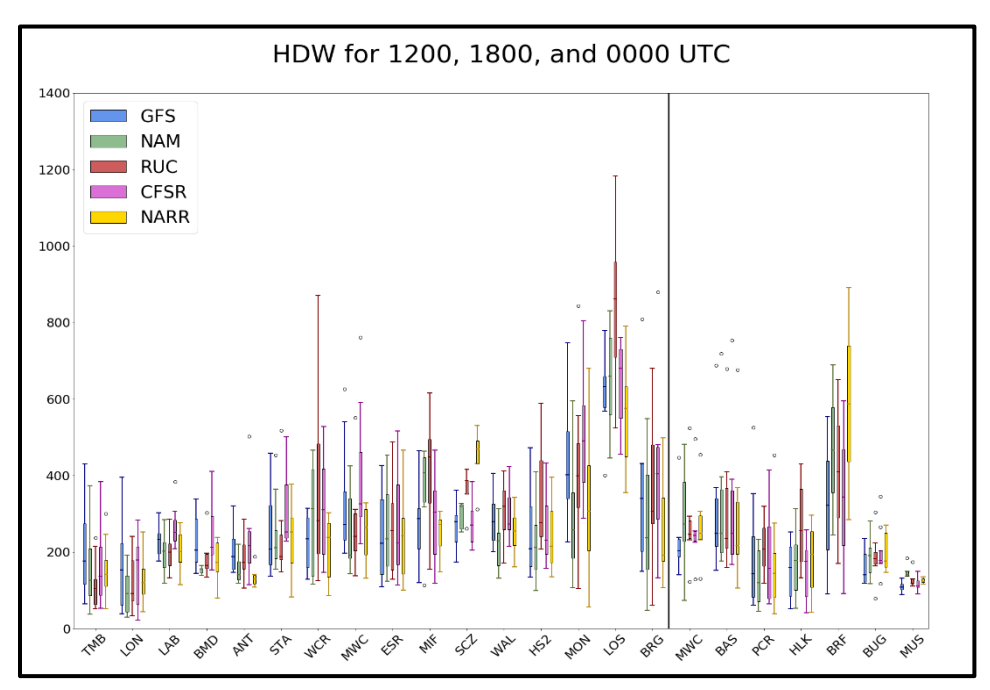


Figure 5: HDW values for all meteorological datasets and wildland fire events during a 11-day period centered on the largest fire spread day. The black line separates western fire events from central and eastern fire events

The successfulness of HDW at identifying the largest spread day for each wildland fire event and each meteorological analysis datasets is presented in Fig. 6. White boxes indicate that HDW maximized on the day of or one day prior to the largest spread day; pink boxes indicate that HDW maximized two or more days prior to and green boxes indicate that HDW maximized one or more days after the largest spread day. The percentage of HDW successes for each analysis dataset appears to the right of the plot; this percentage is used to indicate HDW skill The CFSR exhibited the highest skill with the percentage of 78.2, while the GFS exhibited the lowest skill with the percentage of 56.5. The NARR and RUC analysis datasets all show the same skill percentages of 65.2 for these twenty-three fire events, and the NAM shows a percentage of 60.8. Once again, there is no clear east-west pattern in the successes and failures of HDW, nor are there clear influences of elevation or indications of regional biases in any of the analysis datasets.

However, there is a greater tendency for HDW maximum values to occur after rather than prior to the largest fire spread day in the western United States. This tendency could be due to the effects of local environmental factors affecting the fire events, the influence of complex terrain, or due to temporal errors in the forecast models that are used in the process of producing the analyses (e.g. Colle et al. 2001).

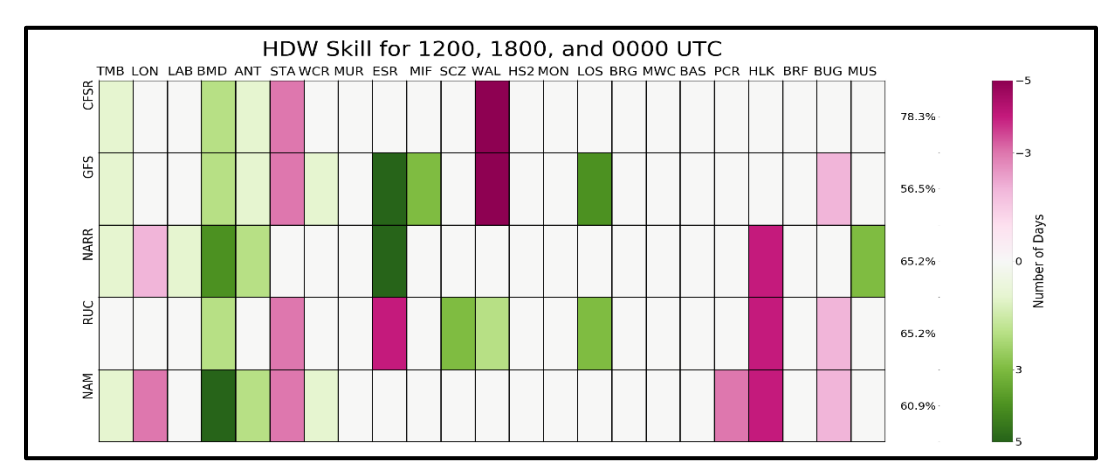


Figure 6: HDW skill for all of the meteorological analysis datasets and wildland fire events. White boxes indicate HDW success, and colored boxes indicate unsuccess. Hit rates are also provided

These results demonstrate that HDW when calculated using the original formulation is able to identify the largest spread day on more than 55% of these wildland fire events for all the meteorological analysis datasets. The question remains of whether modification of HDW formulation, as described in the methods section, could enhance HDW skill. The twenty-three wildland fire events used in this study enables the evaluation of assumptions made during the formulation of the index. This study will now evaluate two of the assumptions made by Srock et al. (2018) in developing HDW: 1) that a 500-m deep layer accounts for the weather conditions that are most likely to interact with a wildland fire during a burning period; 2) that using 1200, 1800, and 0000 UTC is sufficient to account for the burning period of a day for the continental

United States. This investigation will evaluate the extent to which HDW skill depends upon these two assumptions. Two studies of the sensitivity of HDW to layer depth, three studies of the sensitivity of HDW to temporal resolution and range, and six sensitivity studies that combine layer depth and temporal resolutions and range are conducted. For these sensitivity analyses, the control is assumed to be the results from the HDW formulation that appear in Fig. 6.

4.3 Layer Depth Sensitivities

The sensitivities of HDW skill to using deeper atmospheric layers are presented. Specifically, the analysis in Fig. 5 is completed for layer depths of 1000 and 1500 m and the results are compared with the control (Table 3). The peach colors represent percentages that have decreased in comparison to the control analyses, the grey shows the percentages that remain unchanged, and green colors will indicated percentages that increase. The NARR, RUC, and NAM exhibited no change in HDW skill for formulations using the 1000-m layer, while the CFSR and GFS both decreased in skill using the 1000-m layer. For the 1500-m layer, all of the analysis datasets exhibited decreases in HDW skill. These results suggest that increasing the depth of HDW to 1000 m and 1500 m has no positive impact on HDW skill for all of the analysis datasets, and in fact only exhibit negative changes in HDW skill when a change occurs.

Table 3: The percentages of HDW successes for all wildland fire events using 1000-m and 1500-m layer depths to compare with the control analyses

HDW Percent Success (%)						
Analysis Datasets	CFSR	GFS	NARR	RUC	NAM	
500-m Layer (Control)	78.2	56.5	65.2	65.2	60.8	
1000-m Layer	47.8	43.5	65.2	65.2	60.9	
1500-m Layer	52.2	47.8	56.5	47.8	56.5	

4.4 Temporal Sensitivities

The sensitivities of HDW skill to using the maximum available temporal resolution available for each analysis dataset are presented in Table 4 along with the control HDW skill values. Specifically, the analysis in Fig. 5 is repeated using the 1-hour temporal resolution of the RUC and the 3-hour temporal resolution of the NARR for the period beginning at 1200 UTC and ending at 0000 UTC, and the results are compared with the control. Note that the maximum temporal resolution for the CFSR, GFS and the NAM is 6-hour, meaning the skill has to be the same as the control. Using the maximum RUC and NARR temporal resolution increases the potential for larger maximum daily HDW values. Based on the results presented in this table, including all of the available times for each analysis dataset in the calculation of HDW decreased the HDW skill for the NARR to 60.8. This formulation of HDW increased HDW skill for the RUC to 69.5. The decrease of the NARR dataset HDW skill is 4.4 and the increase to the RUC dataset HDW skill is 4.3. An interesting observation of the similarity these differences share in magnitude from the control appear. The evaluation of HDW formulation sensitivity to the addition of 0600 UTC are discussed below and shown in rows 5 and 6.

Table 4: The percentages of HDW successes for all wildland fire events when using all available analysis dataset hours to compare with the control analyses

HDW Percent Success (%)							
Analysis Datasets	CFSR	GFS	NAR	RUC	NA		
			R		M		
12, 18, 00 (Control)	78.2	56.5	65.2	65.2	60.8		
12, 18, 00 (All Hours)	-	-	60.8	69.5	-		
12, 18, 00, 06	65.2	65.2	56.5	52.1	52.1		
12, 18, 00, 06 (All Hours)	-	-	56.5	60.8	-		

With the addition of 0600 UTC to the control, all of the analysis datasets experienced a decrease in percentages of HDW skill except for the GFS, which increased by 9.3 percent. These

results indicate that HDW skill does not show overall improvement to all the datasets. This addition only improves the GFS analysis dataset making evident the need to evaluate the GFS further using more fire events to indicate if the use of 0600 UTC more often than not improves its HDW skill.

Additionally, the sensitivities of HDW skill for each analysis dataset when using all available times between 1200 and 0600 UTC for each analysis dataset are provided in Table 4. Once again, the CFSR, GFS, and NAM do not provide more times than the previous investigation and their percentages remain unchanged. Both the NARR and the RUC exhibit decreases in HDW skill with the addition of higher temporal resolution to the period beginning at 1200 UTC and ending at 0600 UTC. The increase of temporal resolution for the NARR doesn't change from the HDW skill calculated using the times 1200, 1800, 0000, and 0600. Based on these analyses, adding 0600 UTC to the control analysis times decreases HDW skill for all of the analysis datasets except the GFS, requiring further validation of the use of 0600 UTC for this particular analysis dataset using additional fire events.

4.5 Combination of Layer Depth and Temporal Sensitivities

The sensitivities of HDW skill to using combinations of deeper layers and the different temporal resolutions and ranges available for each analysis dataset are additionally presented in Table 5 to the information provided in Table 3 and Table 4. The only positive impact to HDW skill using these combinations is for the first combination of a 1000-m deep layer with all available dataset times between 1200 and 0000 UTC used in formulating HDW. This combination resulted in the RUC analysis dataset being the only dataset to show an increase of 4.4 in HDW skill. This increase is the due to the sensitivity of HDW formulation to the addition of all possible analysis dataset hours between 1200 UTC and 0000 UTC because the sensitivity

of HDW skill to a 1000-m deep layer provided no change in index skill. The combination of these two sensitivities show the same increase in HDW skill as this temporal sensitivity shows. The overall analysis of these sensitivities in HDW formulation suggest that adjustments to the layer depth and temporal resolution does not improve HDW skill for these twenty-three fire events.

Table 5: Percentages of HDW successes for all wildland fire events for the sensitivities of HDW

HDW Percent Success (%)					
	CFS R	GFS	NAR R	RUC	NA M
Control	78.3	56.5	65.2	65.2	60.9
12, 18, 00 (All Hours)	-	-	60.8	69.5	-
12, 18, 00, 06	65.2	65.2	56.5	52.1	52.1
12, 18, 00, 06 (All Hours)	-	-	56.5	60.8	-
1000-m Layer (12, 18, 00)	47.8	43.4	65.2	65.2	60.8
1500-m Layer (12, 18, 00)	52.1	47.8	56.5	47.8	56.5
1000-m Layer (All Hours 12 – 00)	-	-	60.8	69.5	-
1500-m Layer (All Hours 12 – 00)	-	-	43.4	65.2	-
1000-m Layer (12, 18, 00, 06)	39.1	52.1	47.8	60.8	52.1
1500-m Layer (12, 18, 00, 06)	47.8	52.1	39.1	52.1	56.5
1000-m Layer (All Hours 12 – 06)	-	-	47.8	60.8	-
1500-m Layer (All Hours 12 – 06)	-	_	30.4	56.5	-

5. Discussion and Conclusion

The objective of this study is to provide information to fire-weather forecasters, IMETs, and fire managers to facilitate the interpretation of HDW, aiding the implementation of the index into operations. To accomplish this objective, the ability of HDW to identify the largest fire spread day for twenty-three fire events using meteorological data provided by five meteorological analysis datasets is evaluated. Furthermore, this study conducted sensitivity analyses to test the assumptions made by the developers during the formulation of HDW. The

sensitivities to layer depth, temporal resolution, and to combinations of both layer depth and temporal resolution are analyzed.

Based on this evaluation of HDW skill, the index as defined in Srock et al. (2018) is able to identify the largest fire spread day for more than 55% of all the wildland fire events in this study, regardless of the analysis dataset used. No clear difference in performance between forecast analysis datasets and reanalysis datasets is observed. It is shown that there is a greater tendency for maximum HDW values during events in the western US to occur after the largest fire spread day. However, this conclusion could be affected by the greater number of western fire events available for this study. The sensitivity analyses revealed that adjusting the layer depth and temporal resolution does not improve HDW skill for these fire events. However, the results suggest that the effect of combing deeper layers and higher temporal resolution can lead to unpredictable impacts on HDW skill.

The next step to further evaluate HDW skill should be conducted using forecast data for each of the GFS, NAM, and RUC datasets. Additionally, since the NARR exhibited more skill than all of the forecast model analysis datasets, a climatology of HDW using data from the NARR should be produced and compared with the CFSR climatology and other analyses and forecasts. Further evaluation of the impact on HDW skill of complex terrain, proximity to land-sea boundaries, and other orographic affects should be conducted. Evaluations that use additional meteorological datasets with finer grid spacing, higher temporal resolution, and more vertical levels (particularly near the ground) should be investigated for HDW skill. These evaluations could also inform how often conditions suggested by daily HDW values occur at the surface and affect wildland fire behavior.

CHAPTER IV – SUPPLIMENTARY RESULTS

1. Nine-Grid-Point Sensitivity to the Control

Expanding on the control analysis, Fig. 7 shows a grid containing eight additional grid points for each meteorological analysis dataset surrounding the grid points shown in Fig. 6, to investigate the horizontal spatial variability of HDW skill in the vicinity of the fire. This analysis was motivated by the desire to establish attributions for the changes in HDW skill found in the initial sensitivity studies from Chapter III, Section 3. As in Fig. 6, a white box indicates a success and a colored box indicates an unsuccessful HDW identification due to the index maximum value occurring before (pink) or after (green) the largest spread day. The summation of all the white boxes is divided by the summation of the total number of boxes for each analysis dataset to calculate the percentages of HDW success; these percentages appear to the right of the grid for each dataset. The percentages are used to indicate HDW skill for each meteorological analysis dataset.

In this expanded analysis, the CFSR exhibits the highest skill with a percentage of 69.5, while the GFS exhibits the lowest skill with a percentage of 58.9. The NARR shows a skill of 65.2, the RUC shows a skill of 60.8, and the NAM shows a skill of 61.3. As with the central grid point analysis (c.f. Fig. 6), there is no clear east-west pattern in the successes and failures of HDW, nor are there clear influences of elevation or indications of regional biases in any of the analysis datasets. However, nine-point analysis supports the assertion that there is a greater tendency for HDW maximum values to occur after rather than prior to the largest fire spread day in the western US. These results demonstrate that when the surrounding grid points are

considered to the evaluation of HDW skill, the GFS and RUC exhibit increases between one and five percent, while skill decreases for the rest of the analysis datasets.

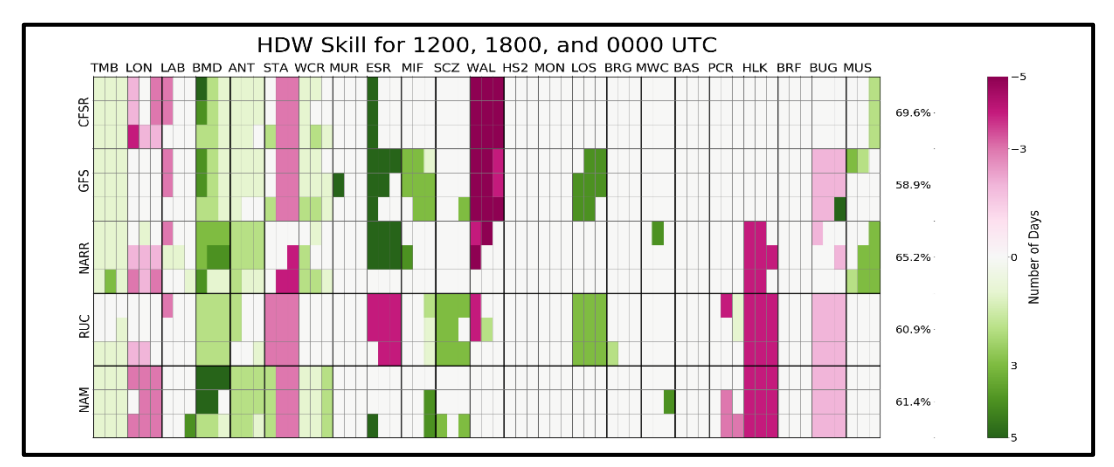


Figure 7: The expansion of the plots presented in Fig. 6 to include the eight grid points surround the central grid point

2. Layer Depth Sensitivities

2.1 Central-Grid-Point Analyses

Section 4.3 in Chapter III analyzed HDW skill using 1000-m and 1500-m deep layers for the central grid point. The analysis that appears in Fig. 5 for the control is now reproduced to show the skill of HDW when calculated using 1000-m (Fig. 8) and the 1500-m (Fig. 9) deep layers. Using a deeper layer causes some fire events to be recategorized as HDW successes and others to be recategorized as unsuccesses, and these changes are different for each analysis dataset.

For example, using the 1000-m deep layer the CFSR doubled or more than doubled the number of unsuccesses due to the day minus two or more and day plus one or more unsuccesses. The GFS shows an increased number of unsuccesses due to an increase to the number of days the index identified days prior to the largest fire spread day. The NARR shows that the Mustang Corner fire event is added to the number of successes while the Monument fire event is recategorized as unsuccessful. The RUC shows that the Shultz fire event is added to the number

of successes while the Tumblebug fire event is recategorized as unsuccessful. The NAM added the Lonesome and Pagami Creek fire events to the number of HDW successes while subtracting the Shultz and Wallow fire events. For some fire events and analysis datasets, the maximum HDW shifted from either after to before or from before to after the maximum spread day. When using a 1500-m deep layer, the CFSR and GFS both had an increase in the number of successes by one: the CFSR added two fire events and lost one, while the GFS added one fire event. All of the other analysis datasets had a net loss of fire events added to the successes, due to a combination of gains and losses of fire events. Evaluation of the effect on HDW skill of these layer dpeths for the surrounding grid points is provided below.

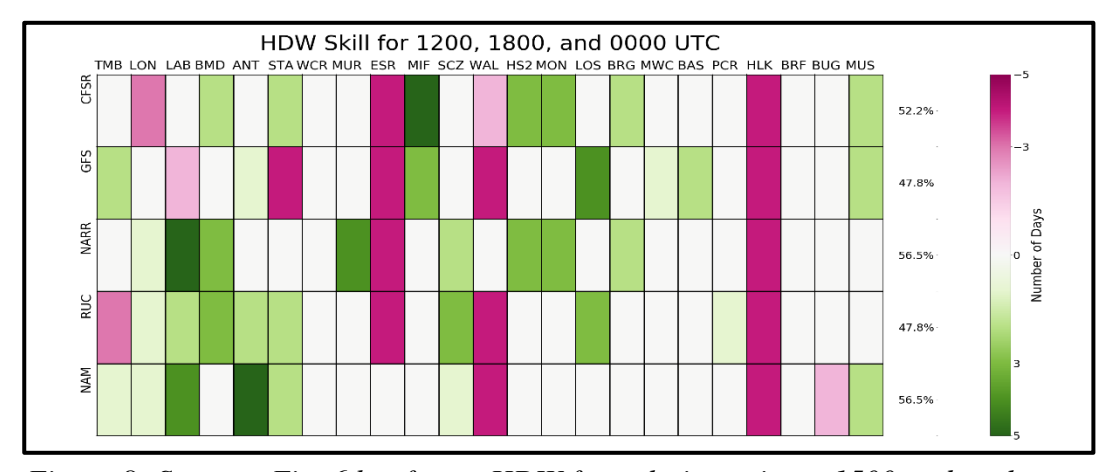


Figure 8: Same as Fig. 6 but for an HDW formulation using a 1500-m deep layer

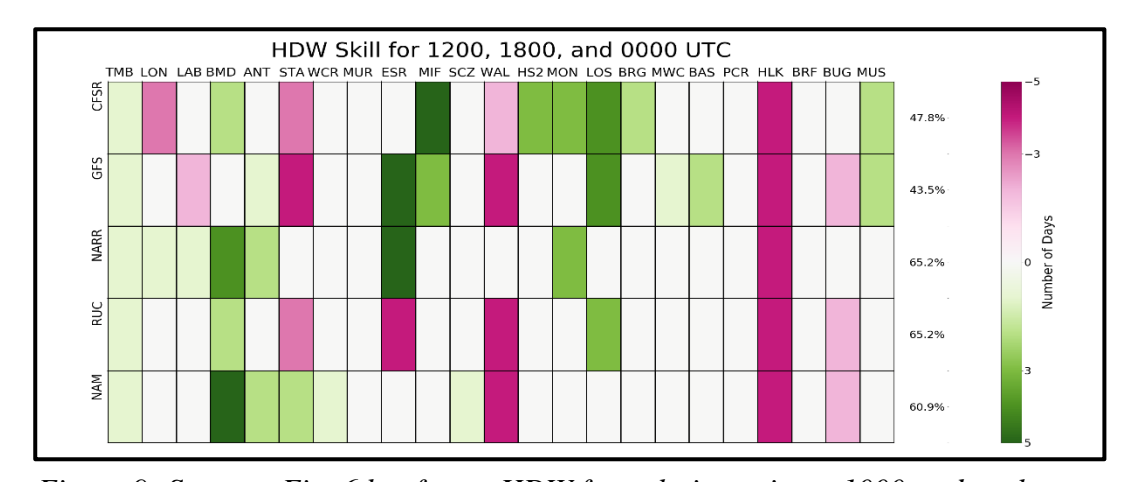


Figure 9: Same as Fig. 6 but for an HDW formulation using a 1000-m deep layer

2.2 Nine-Grid-Point Analyses

The nine-point analysis shown above in Fig. 7 is now reproduced for 1000-m (Fig. 10) and 1500-m (Fig. 11) layer depths. In the analysis of the 1000-m layer depth, the NARR exhibits the highest skill with a percentage of 64.7, while the GFS exhibits the lowest skill with a percentage of 39.1. The CFSR shows a skill of 53.1, the NAM shows a skill of 62.3, and the RUC shows a skill of 56.5. The NAM is the only analysis dataset to show an increase in HDW skill when using a 1000-m layer depth, while the rest of the datasets show decreases in skill compared to the control nine -point analysis (Fig. 7). The NARR, NAM, and RUC show differences of 0.5, 1.0, and 4.4, respectively; the CFSR and GFS show differences of 16.4 and 19.8, respectively. The larger horizontal grid spacing for the CFSR and GFS (Table 1) compared to the other analysis datasets could account for some of these differences in HDW skill. For the 1500-m layer depth analysis (Fig. 11), the highest skill is exhibited by the NAM (56.5), and the lowest skill is exhibited by the GFS (45.4). The other analysis datasets exhibit HDW skills between 53.1 and 54.1. All of the datasets show a decrease in HDW skill compared to the control nine-point analysis. The RUC has the smallest difference in skill (7.7), while the other datasets vary between 11.1 and 15.4.

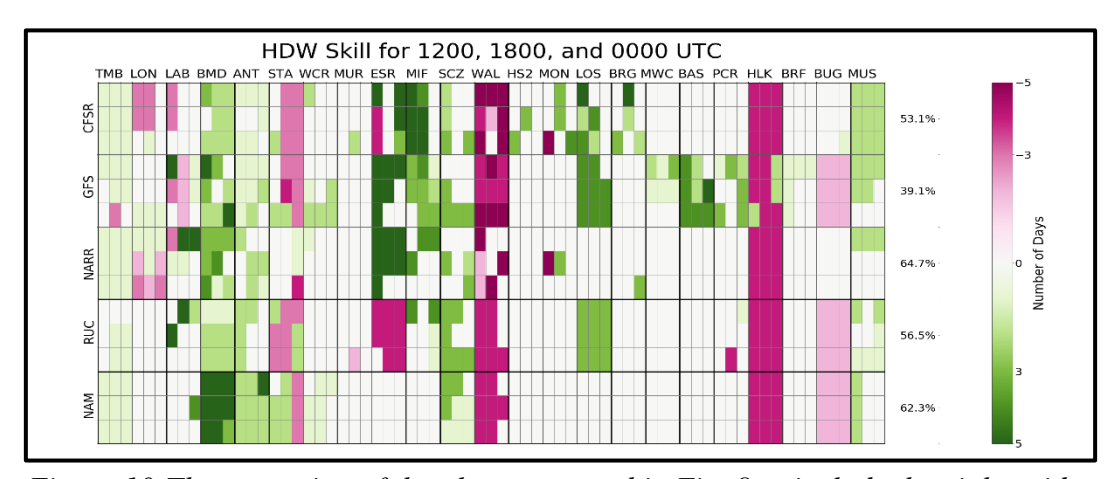


Figure 10:The expansion of the plots presented in Fig. 8 to include the eight grid points surround the central grid point

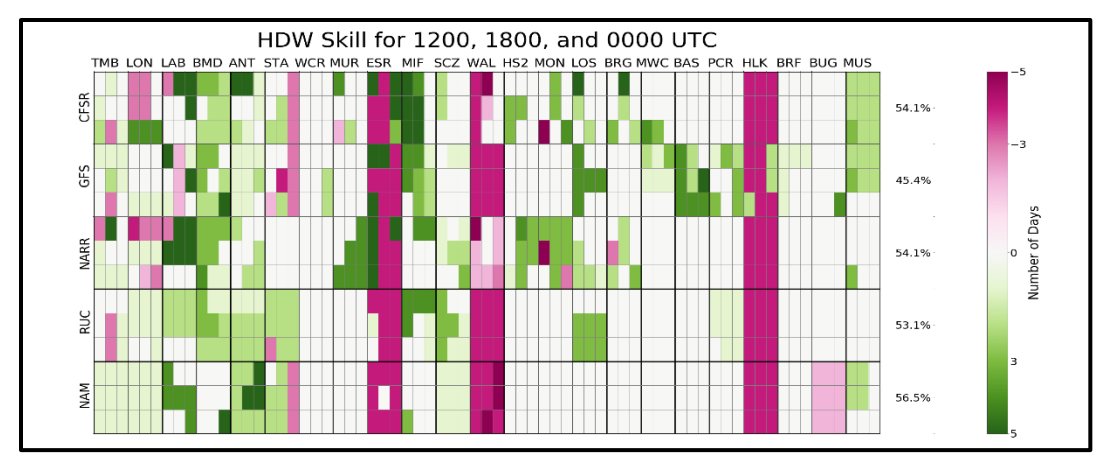


Figure 11: The expansion of the plots presented in Fig. 9 to include the eight grid points surround the central grid point

3. Temporal Sensitivities

3.1 Central-Grid-Point Analyses

Section 3.3 analyzed HDW skill for the central grid point with the addition of 1.) all available analysis dataset times between 1200 and 0000 UTC (Fig. 12); 2.) 1200, 1800, 0000, and 0600 UTC(Fig. 13); and 3.) all available analysis times between 1200 and 0600 UTC(Fig. 14). The analysis that appears in Fig. 5 for the control is now reproduced to show the skill of HDW when calculated using alternative times from the control. Only the NARR and RUC have additional analysis dataset times that can cause HDW from some fire events to be recategorized as HDW successes and others to be recategorized as unsuccesses, and these changes are different for each analysis dataset.

For example, using the addition of all available times between 1200 UTC and 0000 UTC (Fig. 12) from each analysis dataset the NARR decreased in HDW skill by 4.4 to 60.8 while the RUC increased in skill by 4.4 to 69.5. The NARR decreased because of the Milford Flat fire event becoming a unsuccess for HDW. The RUC increased to due to the addition of the Wallow and Lonesome fire events to the number of HDW successes, and the loss of the Bridger fire

event to becoming an HDW unsuccess. The distribution of the timing of HDW identifications of largest fire spread days remains unchanged from the control.

When 1200, 1800, 0000, and 0600 (Fig. 13) are used to formulate HDW, the skill of the index dropped between 8.7 and 13.1 for all of the analysis datasets except for the GFS which increased by 8.7 to 65.2. The CFSR droped due to the loss of Lonesome, La Brea, and Los Conchas fire events to the number of successes. The GFS had a net gain due to the loss of the Lonesome fire event to the number of successes which is countered by the gain of the Milford Flat, Witch Creek, and Los Conchas fire events. The RUC recategorized the Lonesome, Milford Flat, and Pagami Creek fire events as unsuccesses, while the NAM recategorized the La Brea and East Slide Rock Ridge fire events as unsuccesses.

Expanding upon the analysis in Fig. 13, Fig. 14 shows HDW skill when all available analysis dataset times between 1200 UTC and 0600 UTC are used to calculate index values. Once more, the only analysis datasets with higher temporal resolution than the previous analysis are the NARR and RUC. This analysis indicates that both the NARR and the RUC decrease in HDW skill from the control by 8.7 and 4.4 to 56.5 and 60.8, respectively. The NARR recategorized the La Brea fire event as a success and the Murphy, Milford Flat, and Los Conchas fire events as unsuccesses. The RUC recategorized the Wallow fire event as a success and the Lonesome, Murphy, Milford Flat, and Los conchas fire events as unsuccesses.

Although the fire events identified as successful or unsuccessful has shifted, the timing of HDW maximum in relation to the largest fire spread day remains in the same category, although it may have a different magnitude. The overall skill of HDW in the temporal sensitivity analyses for these analysis datasets is lower than the control analysis, suggesting that an increase in

temporal resolution and range does not improve the ability of HDW to indentify the largest spread day for these twent-three wildland fire events.

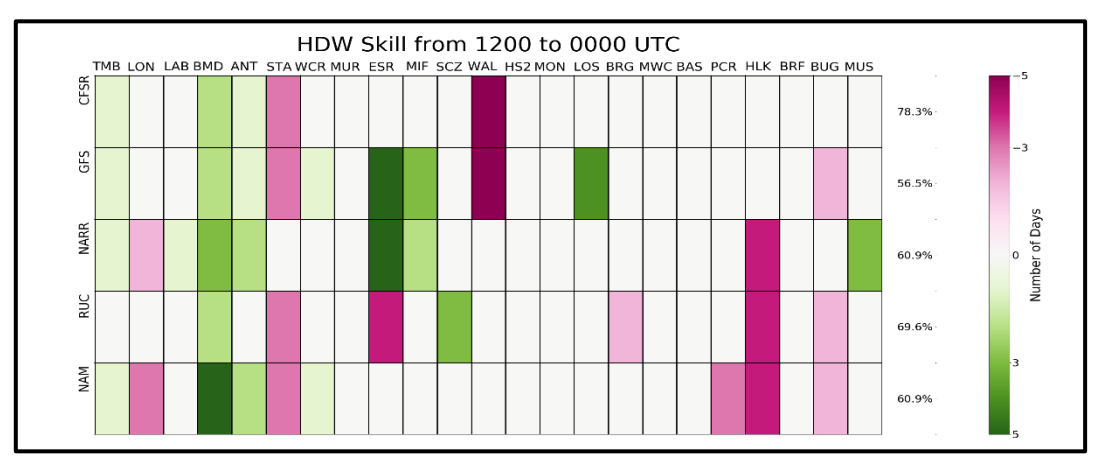


Figure 12: Same as Fig. 6 but for an HDW formulation using all available analysis dataset hours between 1200 UTC and 0000 UTC

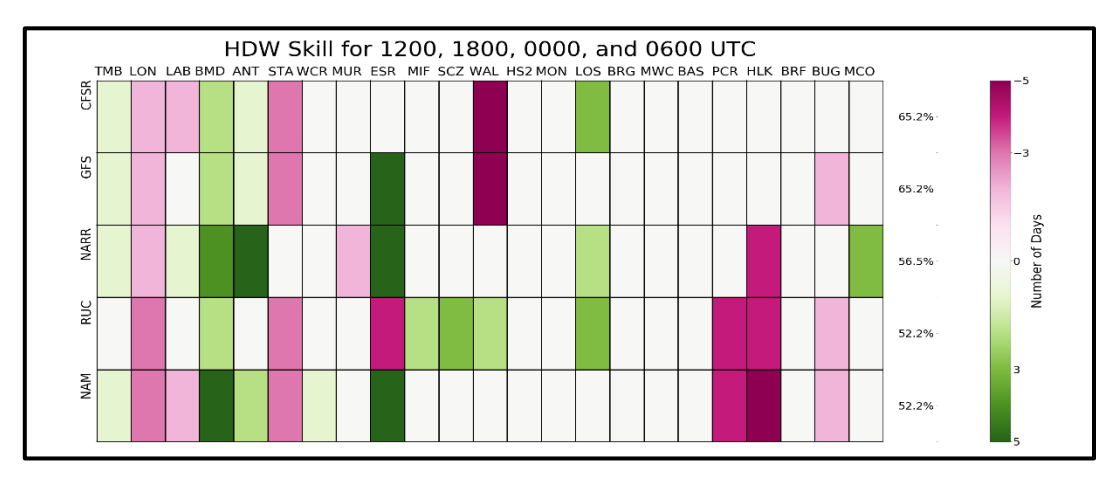


Figure 13: Same as Fig. 6 but for an HDW formulation using all available analysis dataset hours between 1200 UTC and 0600 UTC

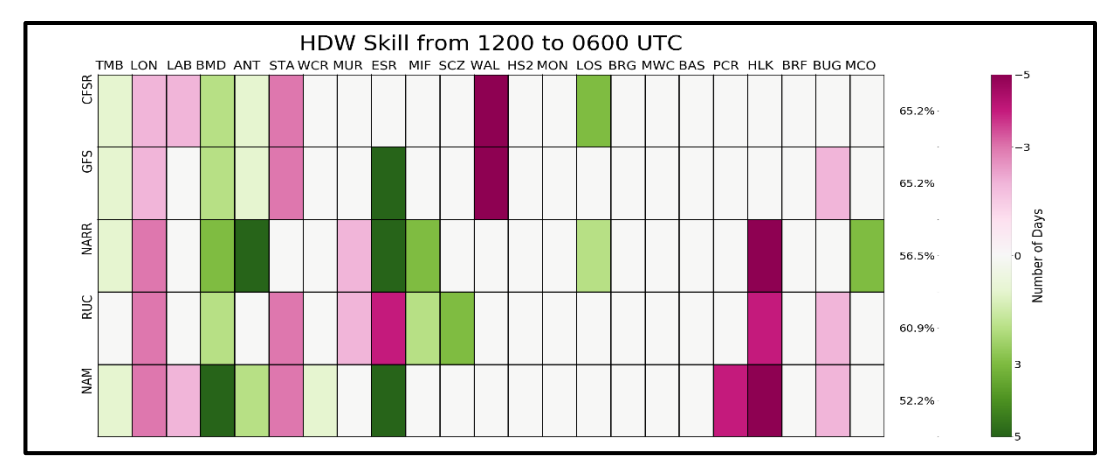


Figure 14: Same as Fig. 6 but for an HDW formulation using 1200, 1800, 0000 and 0600 UTC

3.2 Nine-Grid-Point Analyses

The nine-point analysis shown above in Fig. 11 is now reproduced for; 1.) all available analysis dataset times between 1200 and 0000 UTC (Fig 15), 2.) 1200, 1800, 0000, and 0600 UTC (Fig. 16), 3.) all available analysis dataset times between 1200 and 0600 UTC (Fig. 17). In Fig. 15 the only datasets that could exhibit a change from the HDW skills presented in Fig. 11 are the NARR and RUC. The NARR analysis dataset exhibited a decrease in HDW skill from the control of 8.7 to 69.5 when all nine grid points are considered, respectively. The RUC increased in skill by 0.5 to 65.7. In Fig. 16, the CFSR maintained the highest HDW skill with a value of 68.6, while the lowest skill is reported for the RUC and NAM of 57.4. The GFS is the only analysis dataset exhibiting an increase in skill with the addition of 0600 UTC of 11.1 to 67.6. The CFSR, NARR, RUC, and NAM decreased in skill between 2.5 and 9.6. The CFSR shows a skill of 68.6, the NARR shows a skill of 63.7, the RUC and the NAM both shows a skill of 57.4 for this analysis. In comparison to the control, the nine-point analysis of the HDW formulation using all available analysis dataset times between 1200 and 0600 UTC in Fig. 17 shows that the NARR HDW skill decreased by 3.4 to 61.8 while the RUC index skill increased by 0.5 to 65.7.

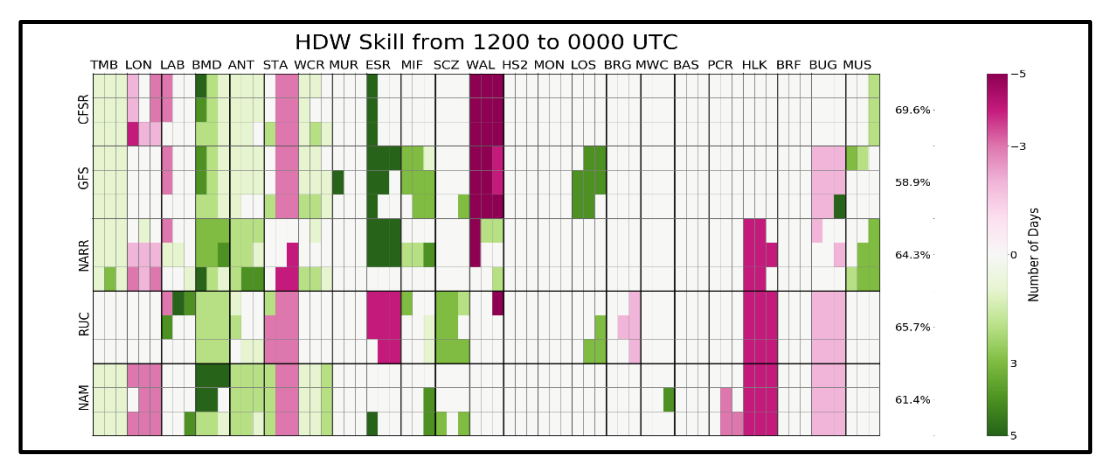


Figure 15: The expansion of the plots presented in Fig. 12 to include the eight grid points surround the central grid point

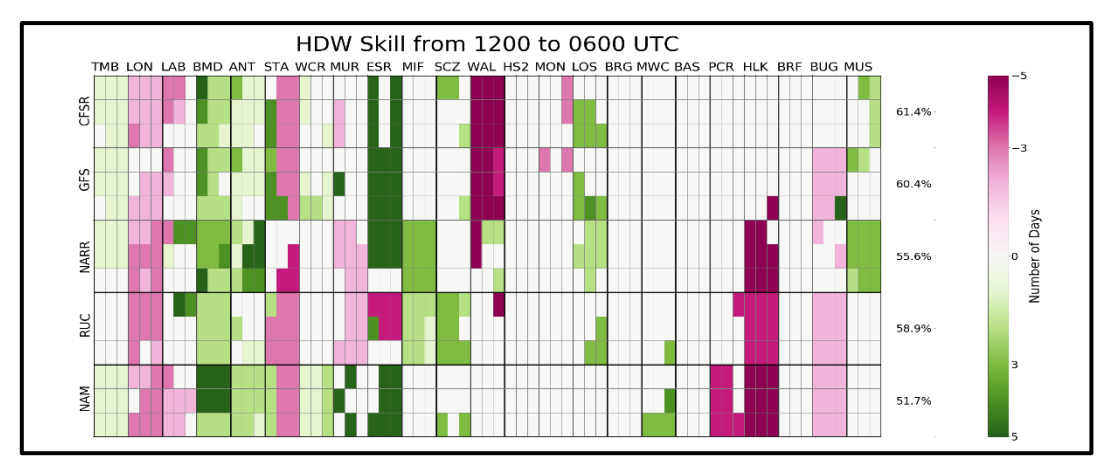


Figure 16: The expansion of the plots presented in Fig. 14 to include the eight grid points surround the central grid point

4. Combination of Layer Depth and Temporal Sensitivities

4.1 Central-Grid-Point Analyses

Section 4.4 analyzed HDW skill for the central grid point using combinations of the sensitivities analyzed above. These combinations include 1.) a layer depth of 1000 m and all available analysis times between 1200 and 0000 UTC (Fig. 18); 2.) a layer depth of 1500 m and all available analysis times between 1200 and 0000 UTC (Fig. 19); 3.) a layer depth of 1000 m and 1200, 1800, 0000, and 0600 UTC (Fig. 20); 4.) a layer depth of 1500 m and 1200, 1800,

0000, and 0600 UTC(Fig. 20); 4.) a layer depth of 1000 m and all available analysis times between 1200 and 0600 UTC(Fig. 21); and 5.) a layer depth of 1500 m and all available analysis times between 1200 and 0600 UTC(Fig. 21). The analysis that appears in Fig. 5 for the control is now reproduced to show the skill of HDW when calculated using alternative layer depths and times from the control. Only the NARR and RUC have additional analysis dataset times which can cause HDW on some fire events to be recategorized as successes or as unsuccesses, and these changes are different for each analysis dataset.

For example, using a layer depth of 1000 m in combination with the addition of all available times between 1200 UTC and 0000 UTC (Fig. 18) from each analysis dataset, all of the datasets except the RUC and NAM resulted in a decrease of HDW skill. The RUC increased by 4.4 to 69.5, while the NAM is unchanged in skill compared to the control. The decreases in HDW skill range from 4.4 to 30.4. The number of fire events recategorized as a success (4) for the RUC is higher than the number recategorized as unsuccesses (3). The CFSR recategorized one fire event as a success, while eight fire events became unsuccesses. The GFS recategorized two fire events as successes and four fire events as unsucesses. The NARR decreased because of one fire event became a success and two fire events became unsuccesses for HDW. Although the NAM remain unchanged in skill from the control analysis, two fire events became successes while two others became unsuccesses. The distribution of the timing of HDW identifications of largest fire spread days remains unchanged from the control.

When using a layer depth of 1500 m in combination with the addition of all available times between 1200 and 0000 UTC (Fig. 19) from each analysis dataset, all except the RUC resulted in a decrease of HDW skill. The RUC exhibits no change in skill from the control. The decreases in HDW skill range from 4.4 to 26.1. Using a 1000-m deep layer and the times 1200,

1800, 0000, and 0600 (Fig. 20) to formulate HDW, the skill of the index dropped between 4.4 and 39.1 for all of the analysis datasets. For a 1500-m deep layer and all available times between 1200 and 0600 UTC (Fig. 21), the skill of HDW dropped between 4.4 and 26.1.

Although the fire events identified as being successful or unsuccessful has shifted, the timing of HDW maximum in relation to the largest fire spread day remains in the same category although it may have a different magnitude. The overall skill of HDW to a combination of layer depths and temporal sensitivity analyses for these analysis datasets is lower than for the control analysis, suggesting that an alternative formulation of HDW does not improve the ability of HDW to indentify the largest spread day on these twenty-three wildland fire events.

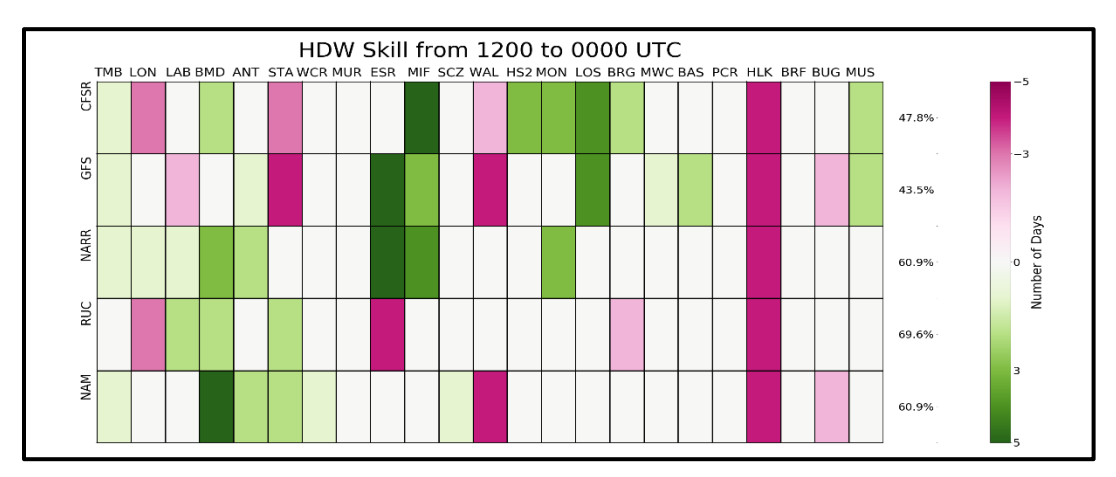


Figure 17: Same as Fig. 6 but for an HDW formulation using a 1000-m deep layer and 1200, 1800, and 0000 UTC

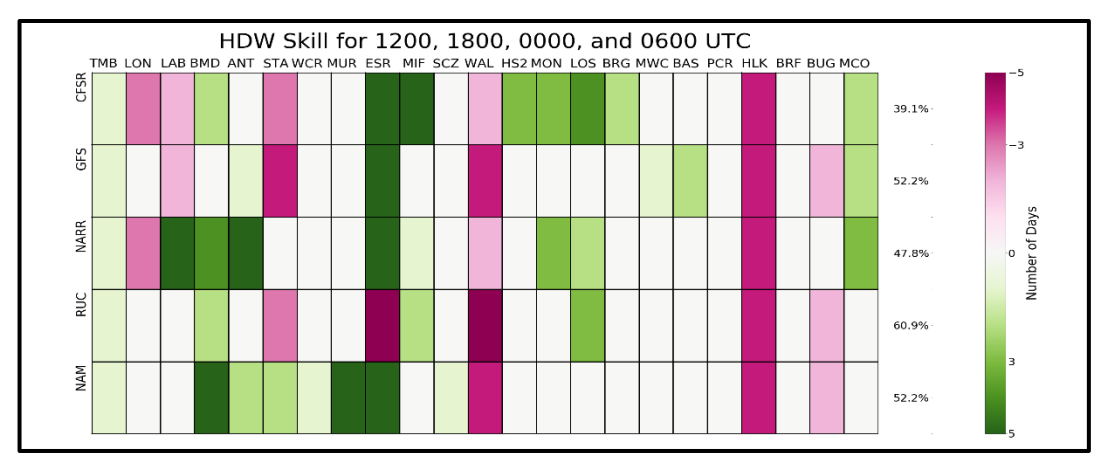


Figure 18: Same as Fig. 6 but for an HDW formulation using a 1000-m deep layer and 1200, 1800, 0000 and 0600 UTC

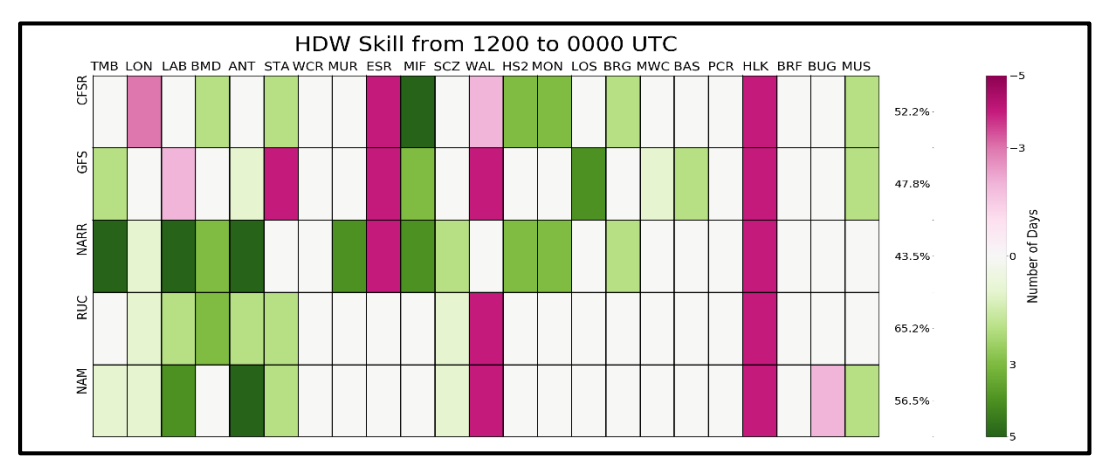


Figure 19: Same as Fig. 6 but for an HDW formulation using a 1500-m deep layer and 1200, 1800, 0000 UTC

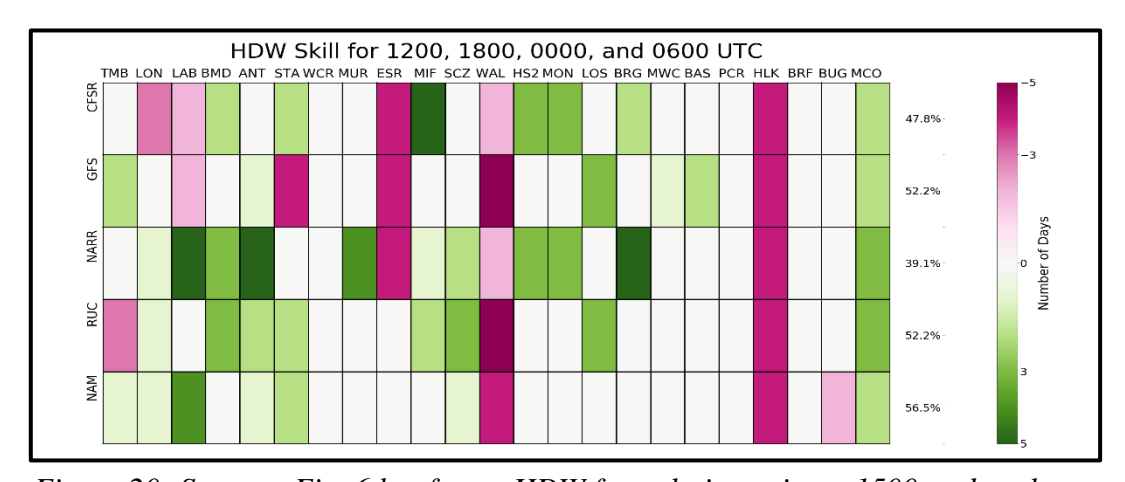


Figure 20: Same as Fig. 6 but for an HDW formulation using a 1500-m deep layer and 1200, 1800, 0000 and 0600 UTC

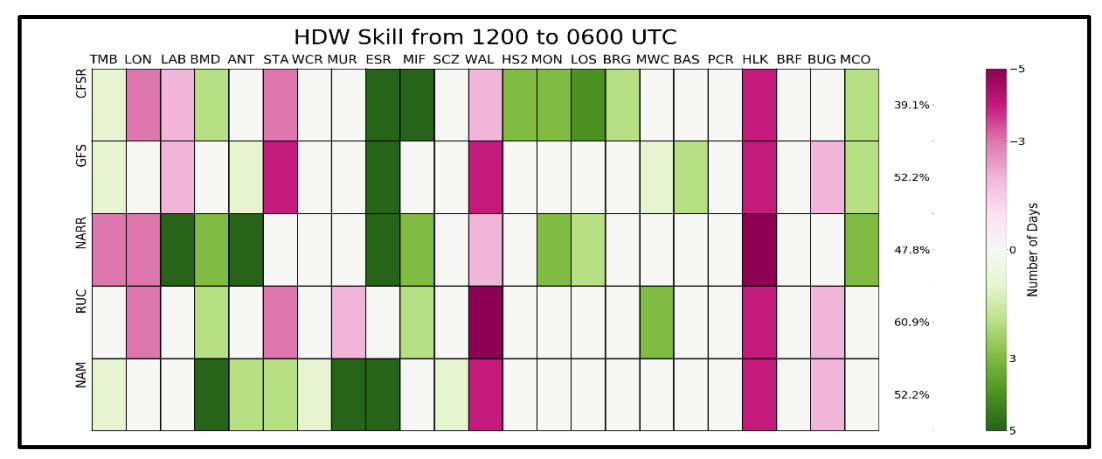


Figure 21: Same as Fig. 6 but for an HDW formulation using a 1000-m deep layer and all available analysis dataset hours between 1200 and 0600 UTC

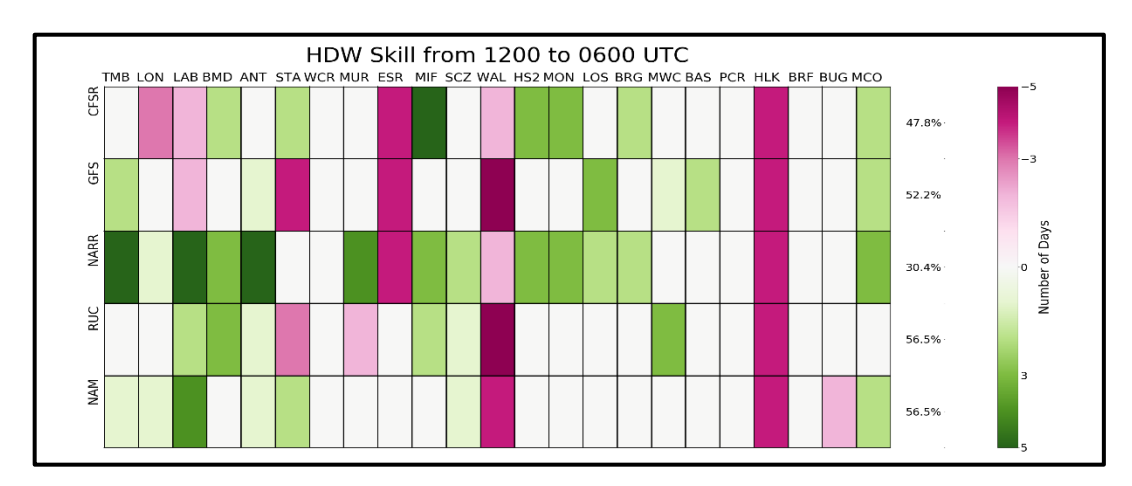


Figure 22: Same as Fig. 6 but for an HDW formulation using a 1500-m deep layer and all available analysis dataset hours between 1200 and 0600 UTC

4.2 Nine-Grid-Point Analyses

The nine-point analysis shown above in Fig. 11 is now reproduced for; 1.) a 1000-m deep layer and all available analysis dataset times between 1200 and 0000 UTC (Fig 22), 2.) a 1500-m deep layer and all available analysis dataset times between 1200 and 0000 UTC (Fig 23), 2.) a 1000-m deep layer and 1200, 1800, 0000, and 0600 UTC (Fig. 24), 3.) a 1500-m deep layer and 1200, 1800, 0000, and 0600 UTC (Fig. 25), 4.) a 1000-m deep layer and all available analysis dataset times between 1200 and 0600 UTC (Fig. 26), and 5.) a 1500-m deep layer and all available analysis dataset times between 1200 and 0600 UTC (Fig. 27). In the Fig. 22 the only

datasets that could exhibit a change from the HDW skills presented in Fig. 11 are the NARR and RUC. The NARR analysis dataset exhibited a decrease in HDW skill from the control of 0.97 to 64.2 while the RUC exhibited an increase in skill of 2.4 to 67.6 when all 9 grid points are considered. In Fig. 22, the RUC now shows the highest HDW skill with a value of 67.6, while the lowest skill is reported for the GFS of 39.1. Figure 23 only differs from fig 22 through the use of a 1500-m deep layer instead of a 1000-m deep layer. In this figure, the NARR analysis dataset exhibited a decrease in HDW skill from the control of 11.6 to 56.6 while the RUC exhibited an increase in skill of 2.4 to 67.6 when all 9 grid points are considered. In Fig. 22, the RUC shows the highest HDW skill with a value of 67.6, while the lowest skill is reported for the GFS of 39.1.

In Figure 24, a 1000-m deep layer is used in conjunction with analysis data for the hours of 1200, 1800, 0000, and 0600 UTC in the formulation of HDW. This analysis shows a decrease for all the meteorological analysis datasets index skill between 1.4 and 25.1. The CFSR decreases in skill to 53.1, the GFS decreases in skill to 48.7, the NARR decreases in skill to 60.8, the RUC decreases in skill to 63.2, and the NAM decreases in skill to 59.4. Figure 25 differs from Fig. 24 by using a 1500-m deep layer instead of 1000-m. In this analysis, the datasets all exhibit decreases, once again, in HDW skill between 1.5 and 20.8. The CFSR skill decreased to 57.4, the GFS decreased to 54.1, the NARR decreased to 48.7, the RUC decreased to 63.7, and the NAM decreased to 57.9.

Figure 26 presents HDW skill based on index formulation using a 1000-m deep layer in conjunction with analysis data for the hours between 1200 and 0600 UTC. This analysis also shows a decrease for all the meteorological analysis datasets index skill between 4.4 and 39.1. The CFSR decreases in skill to 39.1, the GFS decreases in skill to 52.1, the NARR decreases in

skill to 47.8, the RUC decreases in skill to 60.8, and the NAM decreases in skill to 52.1. Figure 27 differs from Fig. 24 by using a 1500-m deep layer instead of 1000-m. In this analysis, the datasets all exhibit decreases in HDW skill between 4.4 and 26.1. The CFSR skill decreased to 52.1, the GFS decreased to 47.8, the NARR decreased to 56.5, the RUC decreased to 47.8, and the NAM decreased to 56.5.

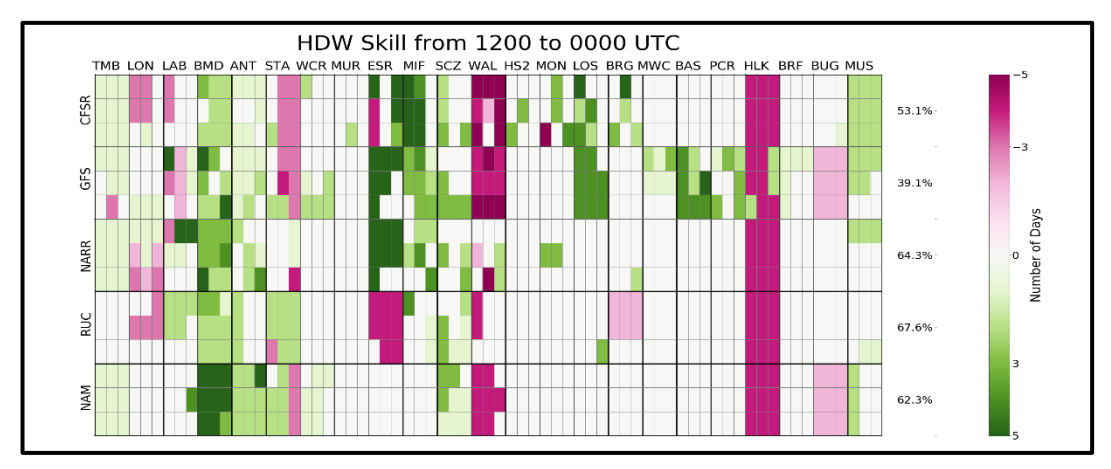


Figure 23: The expansion of the plots presented in Fig. 18 to include the eight grid points surround the central grid point

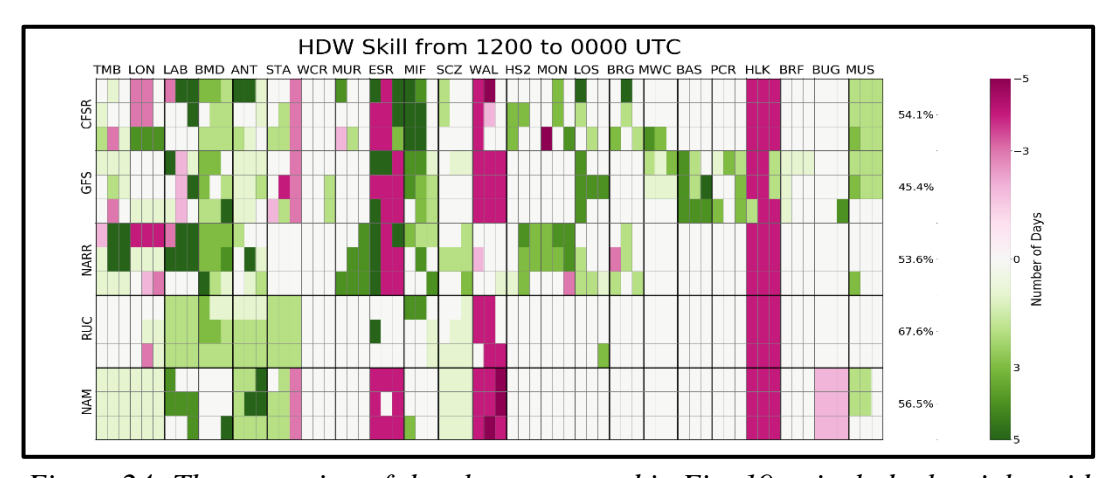


Figure 24: The expansion of the plots presented in Fig. 19 to include the eight grid points surround the central grid point

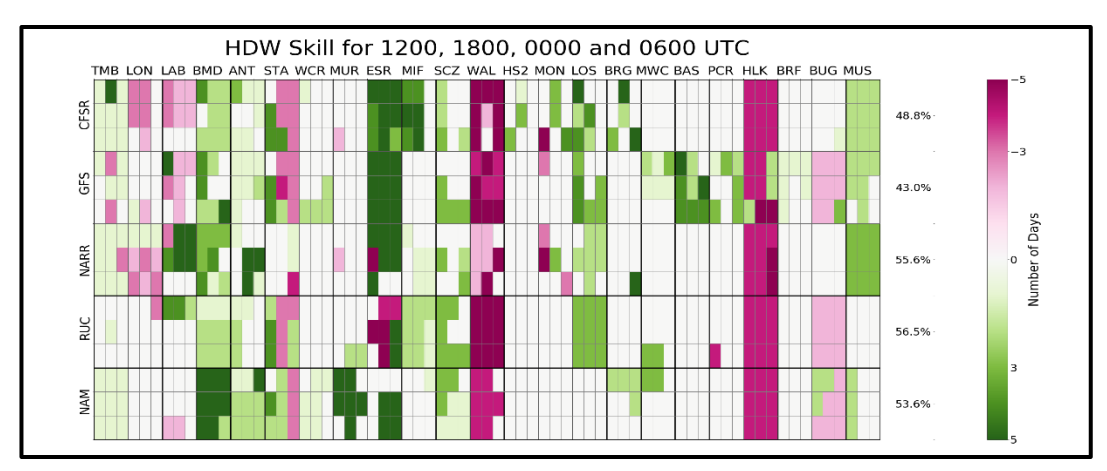


Figure 25: The expansion of the plots presented in Fig. 20 to include the eight grid points surround the central grid point

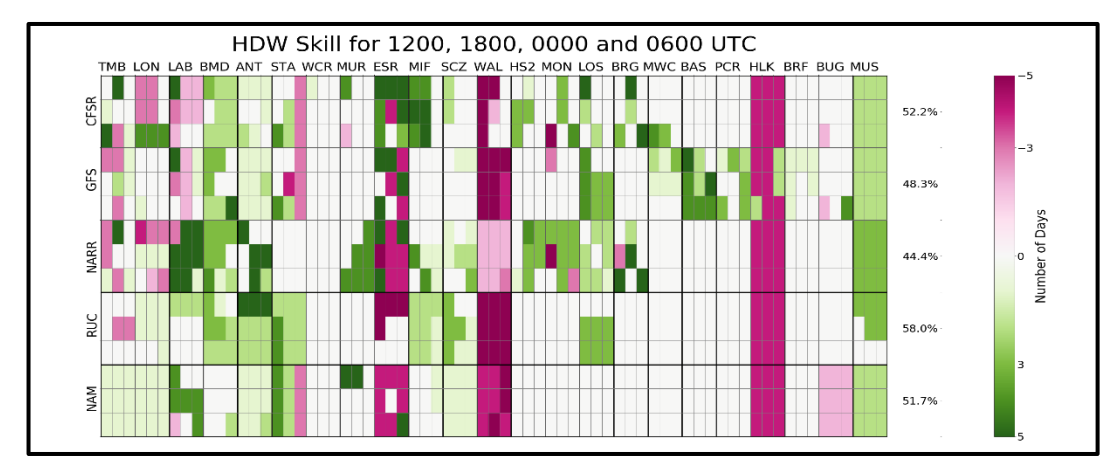


Figure 26: The expansion of the plots presented in Fig. 21 to include the eight grid points surround the central grid point

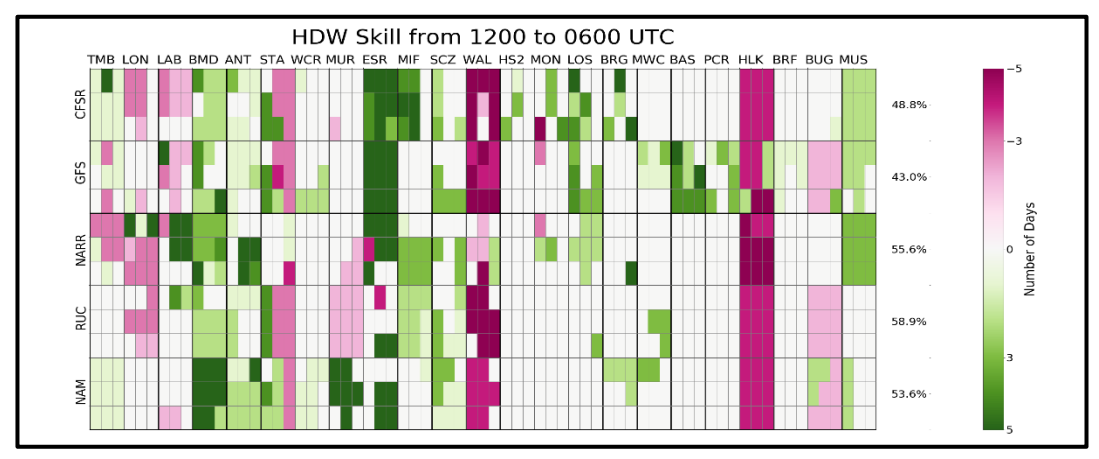


Figure 27: The expansion of the plots presented in Fig. 22 to include the eight grid points surround the central grid point

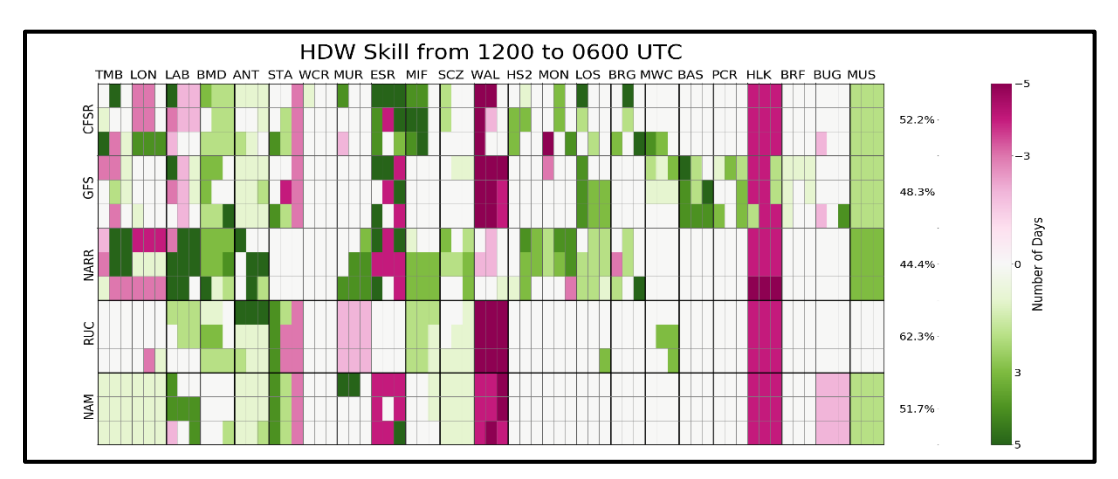


Figure 28: The expansion of the plots presented in Fig. 23 to include the eight grid points surround the central grid point

4.3 Alternative Skill Evaluation of the Nine-Grid-Point Analyses

An additional application of the 9-grid-point analyses is to develop and alternative HDW skill. The alternative skill is calculated by determining when one of the nine grid points is considered an HDW success for each fire event. An HDW unsuccess will now be defined as all of the nine grid points for a fire event being unsuccessful. This analysis will aid in the interpretations of HDW by fire-weather forecasters and IMETs and provide information regarding the potential for locations in the vicinity of a fire to provide higher HDW skill than the central point alone. To conduct these analyses, the newly defined successes are summed and divided by the total number of fire events to produce an alternative skill using the previous 9-grid-point analyses. Table 6 provides the alternative HDW skill using the analyses that appear in the nine-grid-point figures in the previous section.

The alternative control shows an increase for all meteorological analysis datasets over the central-point control (blue row). When comparing the impact of individual sensitivities on the nine-point analysis for the alternative control skill the CFSR shows no changes, while the GFS

shows increases when 1000 m and 1500 m depths are used. The NARR shows a decrease in alternative skill when 0600 UTC is added to the original HDW calculation, and shows an increase when the layer depth is changed to 1500 m. The RUC shows an increase in alternative skill when all hours between 1200 and 0000 UTC are used in the HDW formulation, while a decrease is shown when 0600 UTC is additionally used in the formulation. The NAM shows a decrease when 0600 UTC is used and when a 1500-m deep layer is used in the formulation but shows an increase when a 1000-m deep layer is used.

The impact of the combination of changes in layer depths and temporal resolutions and ranges is shown below the triple line in Table 6. For the CFSR, the combination of a layer depth of 1000 m and the addition of 0600 UTC to the original HDW formulation decreases the alternative skill by 4.4 to 82.6. Conversely, when a 1500-m deep layer is used with the addition of 0600 UTC the CFSR increases by 4.4 to 91.3. The GFS shows no change in alternative skill when combinations are used to formulate HDW, and the NARR decreases for all of the combination formulations of HDW. The NAM increases to 78.3 when the combination of a 1000-m deep layer and 0600 UTC is used and decreases to 60.9 when the layer is 1500 m deep.

Table 6: Alternative percentages of HDW successes for all wildland fire events when using three different temporal ranges depending on temporal resolution of each analysis dataset to compare with the control analyses

Alternative HDW Percent Success (%)						
Analysis Datasets	CFS	GFS	NAR	RUC	NA	
	R		R		M	
Central-Point Control	78.3	56.5	65.2	65.2	60.9	
Alternative Control	87.0	82.6	87.0	78.3	73.9	
12, 18, 00 (All Hours)	-	-	87.0	82.6	-	
12, 18, 00, 06	87.0	82.6	87.0	69.6	69.6	
12, 18, 00, 06 (All Hours)	-	-	78.3	78.3	-	
1000-m Layer (12, 18, 00)	87.0	87.0	87.0	78.3	78.3	
1500-m Layer (12, 18, 00)	87.0	87.0	91.3	78.3	69.6	
1000-m Layer (All Hours 12 – 00)	-	-	82.6	87.0	-	
1500-m Layer (All Hours 12 – 00)	-	-	82.6	78.3	-	
1000-m Layer (12, 18, 00, 06)	82.6	82.6	82.6	69.6	78.3	
1500-m Layer (12, 18, 00, 06)	91.3	82.6	78.3	78.3	60.9	
1000-m Layer (All Hours 12 – 06)	_	-	82.6	78.3	-	
1500-m Layer (All Hours 12 – 06)	_	-	78.3	73.9	-	

CHAPTER V – THESIS CONCLUSIONS

The over-arching objective of this study is to provide information to fire-weather forecasters, IMETs, and fire managers to facilitate the interpretation of HDW, aiding the implementation of the index into operations. To accomplish this objective, the ability of HDW to identify the largest fire spread day for twenty-three fire events using meteorological data provided by five meteorological analysis datasets is evaluated. Furthermore, this study conducted sensitivity analyses to test the assumptions made by the developers during the formulation of HDW. The sensitivities to layer depth, temporal resolution, and to combinations of both layer depth and temporal resolution are analyzed.

The initial results of the evaluation of HDW skill shows that the index is able to identify the largest fire spread day for between 56.5% and 78.2% of the twenty-three wildland fire events in this study, depending on the analysis dataset used. No clear difference in performance between forecast analysis datasets and reanalysis datasets is observed. It is noteworthy that the CFSR and the GFS exhibited the highest and lowest skill, respectively, because the GFS is used as the first guess for the CFSR and both analysis datasets have the same horizontal grid spacing and temporal resolution. The reason for the differences between these two specific datasets should be further investigated. The initial results also show that maximum HDW values tended to occur after the largest fire spread day in the western US. Sensitivity analyses revealed that adjusting the layer depth and temporal resolution did not improve HDW skill for these twenty-three historical wildland fire events. The initial results indicated that the original formulation of HDW exhibited the highest overall skill, although increasing the temporal resolution of the meteorological inputs increased the skill for the RUC, and the addition of 0600 UTC increased the skill for the GFS.

The results from the central grid point analyses provided in Chapter IV expanded on the results in the initial study to show the distributions of HDW skill for the control and each of the sensitivity studies. The motivation of this additional analysis is to establish possible attributions for the changes in HDW skill indicated by the initial results. These additional analyses highlighted the characteristics of the changes in HDW skill and provided more information than the initial evaluations of percentages alone. Specifically, it became evident that some fire events are recategorized as HDW successes and others recategorized as unsuccesses in each of the sensitivity studies, and these changes often differed for each analysis dataset. It is also noted that three of the fire events (LON, WAL, LOS) most often expereinced recategorizations, although no fire event is insensitive to the identified changes.

The nine-point analyses are undertaken to provide additional information about the spatial variability of HDW skill in the vicinity of each fire event. The motivation for these analyses is to identify spatial patterns related to changes in skill and determine if those patterns could be related to specific events or datasets. The results of this analysis, detailed in Chapter VI Section 4, reveal that there are no consistent spatial patterns in the analyses that can be attributed to a single fire event or analysis dataset. In other words, the changes in HDW skill exhibit spatial heterogeneity that does not follow a clear pattern related to changes in HDW formulation. However, the nine-point analyses support the assertion that there is a greater tendency for HDW maximum values to occur after rather than prior to the largest fire spread day in the western US.

An alternative skill is calculated using the nine-point analyses for the twenty-three historical wildland fire events used in this study. This alternative control skill is shown to identify the largest fire spread day for between 73.9% and 87.0% of the fire events, which are higher skills than the central point control skill. An interesting note is that the CFSR shows no

change in alternative skill when the layer depth and temporal resolution and range sensitivities are analyzed individually. However, when the combinations of these sensitivities are used the CFSR shows deviation from the alternative control. The GFS alternative skill increases when layer depths increase, but otherwise remain the same as the alternative control. The NARR shows a decrease in alternative skill for all of the combined sensitivity analyses. The NAM and the RUC show both increases and decreases in alternative skill.

The next step in this investigation is to evaluate HDW skill using forecast data for each of the GFS, NAM, and RUC datasets. Ideally, this evaluation should include investigations of false alarm rates, power of detection, and additional skill analyses that are commonly employed to assess the performance of forecast tools. Additionally, since the NARR exhibited more skill than all of the forecast model analysis datasets, a climatology of HDW using data from the NARR should be produced and compared with the CFSR climatology and other analyses and forecasts. Further evaluation of the impact on HDW skill of complex terrain, proximity to land-sea boundaries, and other orographic affects should be conducted. Evaluations that use additional meteorological datasets with finer grid spacing, higher temporal resolution, and more vertical levels (particularly near the ground) should be investigated for HDW skill. These evaluations could also inform how often conditions suggested by daily HDW values occur at the surface and affect wildland fire behavior.

BIBLIOGRAPHY

BIBLIOGRAPHY

- Abatzoglou, J.T., and Kolden, C.A. 2013. Relationships between climate and macro scale area burned in the western United States. Int. J. Wildland Fire, **22**: 1003–1020. doi:10.1071/WF13019.
- Benjamin, S. G., Dévényi, D., Weygandt, S. S., Brundage, K. J., Brown, J. M., Grell, G. A., ... & Manikin, G. S. (2004). An hourly assimilation—forecast cycle: The RUC. Monthly Weather Review, 132(2), 495-518.
- CA.gov, 2019: CARR FIRE. cdfdata.fire.ca.gov/incidents/incidents_details_info?incident_id=2164.
- California Department of Forestry and Fire Protection. 2017. Tubbs fire incident information. http://www.fire.ca.gov/current_incidents/incidentdetails/Index/1867 (last accessed March 30th, 2018).
- Climate Data Guide. Climate Forecast System Reanalysis (CFSR). 2018. https://climatedataguide.ucar.edu/climate-data/climate-forecast-system-reanalysis-cfsr (accessed on April 25th, 2018).
- CNN WIRE, 2018: Carr Fire Becomes 6th Most Destructive Fire in California State History. https://fox40.com/2018/07/31/carr-fire-in-california-becomes-6th-most-destructive-fire-in-state-history/%0D.
- Colle, B. A., C. F. Mass, and D. Ovens, 2001: Evaluation of the timingandstrengthofMM5andEtasurfacetroughpassagesover the eastern Pacific. Wea. Forecasting, 16, 553–572, doi:10.1175/1520-0434(2001)016,0553:EOTTAS.2.0.CO;2.
- Environmental Modeling Center, 2003: The GFS Atmospheric Model. NOAA/NCEP/Environmental Modeling Center Office Note 442, 14 pp. [Available online at http://www.emc.ncep.noaa.gov/officenotes/FullTOC.html.].
- Fosberg MA (1978) Weather in wildland fire management: the fire weather index. In 'Proceedings of the Conference on Sierra Nevada Meteorology', 19–21 June, Lake Tahoe, CA. pp. 1–4. (American Meteorological Society: Boston, MA).
- Gabert, B., 2015: Fort Collins brewery partners to thin and prescribed burn forest. https://wildfiretoday.com/tag/high-park-fire/.
- Haines DA (1988) A lower atmospheric severity index for wildland fire. *National Weather Digest* **13**(2), 23–27.
- Haines, D.A. A lower atmospheric severity index for wildland fire. *Natl. Wea. Dig.* **1988**, *13*, 23–27.

- Janjic, Z., 1997: Advection scheme for passive substances in the NCEP Eta Model. Research Activities in Atmospheric and Oceanic Modeling, WMO, Geneva, CAS/JSC WGNE, 3.14.
- Janjic, Z., 2003: A nonhydrostatic model based on a new approach. Meteor. Atmos. Phys., 82, 271285.
- Janjic, Z., 2009: Further development of a model for a broad range of spatial and temporal scales. Proc 23rd Conference on Weather Analysis and Forecasting/19th Conference on Numerical Weather Prediction, American Meteorological Society, Omaha, NE.
- Janjic, Z., T. Black, M. Pyle, H.-Y. Chuang, E. Rogers, and G. DiMego, 2005: The NCEP WRF model core. Proc. 21st Conference on Weather Analysis and Forecasting/17th Conference on Numerical Weather Prediction, American Meteorological Society, Washington, DC.
- Langholz H. and E. Schmidtmayer. 1993. Meteorologische Verfaren zur Abschatzung des Waldbrandrisikos. AFZ, Nr. 8.: 394-396.
- McArthur AG (1967) Fire behaviour in eucalypt forests. Department of National Development, Forestry and Timber Bureau Leaflet No. 107. (Canberra, ACT).
- McCaw, L., P. Marchetti, G. Elliot, and G. Reader, 2007: Bushfire weather climatology of the Haines Index in southwestern Australia. Aust. Meteorol. Mag., 56, 75–80.
- McKenzie, D.., Gedalof, Z., Peterson, D. L., and Mote, P., 2004: Climatic Change, Wildfire, and Conservation. Conservation Biology **18**, 890-902, https://doi.org/10.1111/j.1523-1739.2004.00492.x.
- Mesinger, F., DiMego, G., Kalnay, E., Mitchell, K., Shafran, P. C., Ebisuzaki, W., ... & Ek, M. B. (2006). North American regional reanalysis. Bulletin of the American Meteorological Society, 87(3), 343-360.
- Miller, J. D., H. D. Safford, M. Crimmins & A. E. Thode (2008). Quantitative evidence for increasing forest fire severity in the Sierra Nevada and Southern Cascade Mountains, California and Nevada, US. *Ecosystems*, 12, 16-32.
- National Centers for Environmental Prediction, National Weather Service, NOAA, U.S. Department of Commerce, 2010: Climate Forecast System Reanalysis (CFSR), for 1979 to 2011, accessed 06/30/2018, gov.noaa.ncdc:C00765.
- National Wildfire Coordinating Group. Gaining an Understanding of the National Fire Danger Rating System. 2002. htp://www.nwcg.gov (accessed on 5/31/2018)

- Nunes, F., R. Rocha, J. Espinola, J. Menezes, J. Amaral, Marcos, Nascimento, and I. Santos, 2017: Fire Risk Calculation in Serra Do Cabral At Simao Dias-Se, Brazil, Using the Angstrom Index. *Ecosyst. Sustain. Dev.*, **214**, 99–103, doi:10.2495/ECO170101.
- Potter B., 2018: The Hazards of Using Fire Size Data for Research. 12th Fire and Forest Meteorology Symposium. 2018, Boise, ID, Amer. Meteor. Soc.https://ams.confex.com/ams/33AF12F4BG/meetingapp.cgi/Paper/343760.
- Saha, S.; Coauthors. The NCEP Climate Forecast System Reanalysis. *Bull. Amer. Meteor. Soc.* **2010**, *91*, 1015–1057.
- Schlobohm, P., and Brain, P., 2002: Gaining an Understanding of the National Fire Danger Rating System. PMS 932, NFES 2665. 82 pp, https://www.nwcg.gov/sites/default/files/products/pms932.pdf.
- Srock, A., et al., 2015: Investigating Simple Fire Weather Indices Using Reanalysis Data: *11th Symposium on Fire and Forest Meteorology 2015*, Minneapolis, MN, Amer. Meteor. Soc., https://ams.confex.com/ams/11FIRE/webprogram/Paper272183.html.
- Srock, Alan; Charney, Joseph; Potter, Brian; Goodrick, Scott. 2018. The hot-dry-windy index: A new fire weather index. *Atmosphere*. 9(7): 27nine-289. 11 p. https://doi.org/10.3390/atmos9070279.
- Van Wagner CE, 1974: Structure of the Canadian forest fire weather index. Canadian Forestry Service. Publ. 1333.
- Wei, M.; Toth, Z.; Wobus, R.; Zhu, Y. Initial perturbations based on the ensemble transform (ET) technique in the NCEP global operations forecast system. Tellus A 2008, 60, 62–79. [CrossRef]
- Willis, Carla, Brian van Wilgen, Kevin Tolhurst, Colin Everson, Peter D'Abreton, Lionel Pero, and Gavin Fleming. "The development of a national fire danger rating system for South Africa." Department of Water Affairs and Forestry, Pretoria (2001).